MANAGING ATMOSPHERIC CO_2

L. D. DANNY HARVEY
Department of Geography, University of Toronto, 100 St. George Street, Toronto, Canada M5S 1A1

Abstract. A coupled carbon cycle-climate model is used to compute global atmospheric CO_2 and temperature variation that would result from several future CO_2 emission scenarios. The model includes temperature and CO_2 feedbacks on the terrestrial biosphere, and temperature feedback on the oceanic uptake of CO_2. The scenarios used include cases in which fossil fuel CO_2 emissions are held constant at the 1986 value or increase by 1% yr^{-1} until either 2000 or 2020, followed by a gradual transition to a rate of decrease of 1 or 2% yr^{-1}. The climatic effect of increases in non-CO_2 trace gases is included, and scenarios are considered in which these gases increase until 2075 or are stabilized once CO_2 emission reductions begin. Low and high deforestation scenarios are also considered. In all cases, results are computed for equilibrium climatic sensitivities to CO_2 doubling of 2.0 and 4.0 °C.

Peak atmospheric CO_2 concentrations of 400–500 ppmv and global mean warming after 1980 of 0.6–3.2 °C occur, with maximum rates of global mean warming of 0.2–0.3 °C $decade^{-1}$. The peak CO_2 concentrations in these scenarios are significantly below that commonly regarded as unavoidable; further sensitivity analyses suggest that limiting atmospheric CO_2 to as little as 400 ppmv is a credible option.

Two factors in the model are important in limiting atmospheric CO_2: (1) the airborne fraction falls rapidly once emissions begin to decrease, so that total emissions (fossil fuel + land use-induced) need initially fall to only about half their present value in order to stabilize atmospheric CO_2, and (2) changes in rates of deforestation have an immediate and proportional effect on gross emissions from the biosphere, whereas the CO_2 sink due to regrowth of forests responds more slowly, so that decreases in the rate of deforestation have a disproportionately large effect on net emission.

If fossil fuel emissions were to decrease at 1–2% yr^{-1} beginning early in the next century, emissions could decrease to the rate of CO_2 uptake by the predominantly oceanic sink within 50–100 yrs. Simulation results suggest that if subsequent emission reductions were tied to the rate of CO_2 uptake by natural CO_2 sinks, these reductions could proceed more slowly than initially while preventing further CO_2 increases, since the natural CO_2 sink strength decreases on time scales of one to several centuries. The model used here does not account for the possible effect on atmospheric CO_2 concentration of possible changes in oceanic circulation. Based on past rates of atmospheric CO_2 variation determined from polar ice cores, it appears that the largest plausible perturbation in ocean-air CO_2 flux due to changes of oceanic circulation is substantially smaller than the permitted fossil fuel CO_2 emissions under the above strategy, so tieing fossil fuel emissions to the total sink strength could provide adequate flexibility for responding to unexpected changes in oceanic CO_2 uptake caused by climatic warming-induced changes of oceanic circulation.

1. Introduction

The atmospheric concentration of CO_2 and other greenhouse gases is expected to

Climatic Change **15**: 343–381, 1989.

increase significantly over the next few decades and to lead to large and essentially irreversible changes of climate. It is often regarded as an established fact that atmospheric CO_2 concentration will eventually double, the only question being when this doubling will occur. Most recent carbon cycle model studies of possible future CO_2 concentrations assume fossil fuel CO_2 emissions to grow exponentially at rates ranging from 0.3% yr^{-1} to 3.0% yr^{-1} (i.e.: Goudriaan and Ketner, 1984; Trabalka *et al.*, 1986) or assume that the entire recoverable fossil fuel resource will be consumed following a logistic curve (i.e.: Bacastow and Bjorkstrom, 1981; Killough and Emanuel, 1981; Viecelli *et al.*, 1981; Siegenthaler, 1983).

Some studies consider scenarios in which CO_2 emissions decrease (Perry *et al.*, 1982; Laurmannn and Spreiter, 1983; Khandani and Rose, 1985; Perry, 1986; Maier-Reimer and Hasselmann, 1987). Ekdahl and Keeling (1973) had showed that, for an exponential increase of CO_2 emissions with an invariant time constant μ, the airborne fraction (the fraction of emitted CO_2 remaining in the atmosphere) is approximately constant after a few multiples of μ for linear models. Perry (1986) argued that the error introduced by assuming a constant airborne fraction for scenarios in which CO_2 emissions begin to decrease is small, even for scenarios leading to CO_2 ceilings as low as 500 ppmv. However, results of Maier-Reimer and Hasselmann (1987) and discussion by Firor (1988) indicate that the ocean will take up an increasingly larger fraction of emitted CO_2 as emissions decrease, corresponding to a decrease of the airborne fraction.

Numerous studies have shown that substantial reductions in total energy use, and hence in CO_2 emissions, are possible in the industrialized world through improved efficiency of energy use, and that the third world need not follow the industrialized world's path of high energy use as it undergoes development (see Lovins, 1980; Cheng *et al.*, 1986; Goldemberg *et al.*, 1985, 1988; Johansson and Williams, 1987; Chandler, 1988; Johansson *et al.*, 1989; and references therein). In particular, Goldemberg *et al.* (1985, 1988) show that in a world of 7 billion people by 2030, the third world could be brought to a Western European standard of living and the industrialized world's per capita primary energy use reduced by 50%, for an increase of global primary energy demand of only 10%.[1]

Given the tremendous scope for reducing CO_2 emissions below what they would otherwise be by improving energy efficiency, the further decreases possible through increased use of non-fossil fuel energy sources (see Harvey, 1989a), and the tendency of the airborne fraction to decrease as CO_2 emissions decrease, it is pertinent to examine the impact on atmospheric CO_2 concentration of a number of CO_2 emission reduction scenarios. To do this, we use a coupled climate-carbon cycle model which includes the additional forcing attributable to the buildup of other greenhouse gases.

[1] Although total primary energy demand (commercial + non-commercial) increases by only 10%, commercial primary energy demand increases by 30% globally and by 120% in the developing world according to this scenario.

2. Model Description

2.1. *Climate Model*

We use the globally averaged upwelling-diffusion model of Harvey and Schneider (1985), which consists of an atmospheric box, a surface box equivalent to the oceanic mixed layer and a thin slab representing the land thermal inertia, and an advective-diffusive deep ocean. In this model the outgoing infrared emission to space F is parameterized as

$$F = A + BT, \tag{1}$$

where A and B are constants and T is atmospheric temperature. The equilibrium sensitivity of the model to a given radiative perturbation can be controlled by changing the value of B, with a compensating change in A to give the same infrared emission to space for the present global mean temperature. Recent GCM sensitivities for a CO_2 doubling, ΔT_{2x}, range from 2.8 °C (Schlesinger and Zhao, 1989) to 5.2 °C (Wilson and Mitchell, 1987), although an alternative model-based approach suggests that ΔT_{2x} is in the range 2–3 °C (Harvey, 1989b). Here, we use sensitivities of 2 °C and 4 °C, with $A = -376.73$ W m^{-2} and $B = 2.2375$ W m^{-2} K^{-1} for $\Delta T_{2x} =$ 2 °C, and $A = -74.98$ W m^{-2} and $B = 1.1875$ W m^{-2} K^{-1} for $\Delta T_{2x} = 4$ °C.

The radiative forcing due to the buildup of greenhouse gases is imposed by adjusting the parameter A by an amount given below. The climate model is first run to equilibrium with pre-industrial values of all trace gases, then integrated from 1770 to 2200 or 2300 using yearly atmospheric CO_2 values and other trace gas concentrations.

In order to obtain an equally good fit to the historical temperature trend over the past 120 yrs with different values of ΔT_{2x}, different values of the upwelling velocity w and diffusion coefficient K are used for the two sensitivities. For $\Delta T_{2x} = 2.0$ °C, we use $w = 4$ m yr^{-1} and $K = 0.6$ cm^2 s^{-1}, while for $\Delta T_{2x} = 4.0$ °C we use $w = 0$ and $K = 3$ cm^2 s^{-1}, giving a purely diffusion ocean model. Both changes for $\Delta T_{2x} =$ 4.0 °C contribute to a slower transient response when scaled by the equilibrium sensitivity (Harvey, 1986).

2.2. *Carbon Cycle Model*

The carbon cycle model consists of a convolution integral which mimics the oceanic uptake of anthropogenic CO_2 obtained by the Maier-Reimer and Hasselmann (1987) oceanic general circulation model (GCM), a correction for temperature ocean-pCO_2 feedback, and a terrestrial biosphere model which is driven by changes of atmospheric CO_2 and temperature.

Oceanic Uptake of CO_2

For a linear system, the variation of atmospheric CO_2 concentration $y(t)$ as a result

of an emission perturbation $x(t)$ and oceanic uptake of CO_2 can be obtained as the convolution of the emission function with the impulse response $G(t)$ of the ocean to an instantaneous injection of CO_2. That is,

$$y(t) = y(0) + \int_0^t G(t-t')x(t')\,dt' . \tag{2}$$

Maier-Reimer and Hasselmann (1987) computed the impulse response $G(t)$ of their three-dimensional oceanic GCM to the sudden injection into the atmosphere of an amount of CO_2 equal to 0.25, 1.0, and 3.0 of the initial CO_2 amount. $G(t)$ is expressed as a sum of exponentials in the form

$$G(t) = A_0 + \Sigma A_i\, e^{-t/\tau_i}, \tag{3}$$

where $A_0 + \Sigma A_i = 1.0$ and τ_i is the time constant governing the decrease in the fraction A_i of the initially injected CO_2. The A_i and τ_i are given in Table I for the reader's convenience, and can be seen to be similar for injections of 0.25 and 1.0 of the initial CO_2, indicating close to linear response, but differ for an injection of 3.0 times the initial CO_2, as the oceanic ability to absorb CO_2 decreases. Here, atmospheric CO_2 is computed as

$$y(t) = y(0) + \int_0^{t_1} G_1(t-t')x(t')\,dt' +$$

$$+ \int_{t_1}^{t_2} G_2(t-t')x(t')\,dt' + \int_{t_2}^{t_3} G_3(t-t')x(t')\,dt' , \tag{4}$$

where $G_1(t)$, $G_2(t)$, and $G_3(t)$ are the impulse responses for injections of 0.25, 1.0, and 3.0 times the initial CO_2, and t_1 and t_2 are the times at which the cumulative anthropogenic CO_2 emission equals 0.5 and 1.0, respectively, of the preindustrial atmospheric CO_2 content. Time t_1 occurs around the year 2000 for an initial CO_2 concentration of 280 ppmv (590 GT C, 1 GT = 10^9 metric tonnes) with fossil fuel emissions alone, and occurs sooner when net biospheric emissions are included. For most scenarios considered here, time t_2 is not reached, so only the first two integrals of Equation (4) are used. Equation (4) was tested against the published

TABLE I: Coefficients derived from the Maier-Reimer and Hasselmann (1987) oceanic GCM for an impulse CO_2 input to the atmosphere of 0.25, 1.0, and 3.0 times present atmospheric CO_2. See text for explanation

	A_i					τ_i			
CO_2 injection:	0	1	2	3	4	1	2	3	4
0.25 × present	0.131	0.201	0.321	0.249	0.098	362.9	73.6	17.3	1.9
1.0 × present	0.142	0.241	0.323	0.206	0.088	313.8	79.8	18.8	1.7
3.0 × present	0.166	0.356	0.285	0.130	0.063	326.3	91.3	18.9	1.2

response of the full GCM to an injection of 5000 GT C by the year 2400, and gave a peak atmospheric CO_2 concentration of about 1400 ppmv compared to about 1625 for the GCM. For impulse inputs of 0.25 and 1.0 the initial atmospheric CO_2, the convolution integral gives much closer agreement with the GCM response, as indicated in Figure 17 of Maier-Reimer and Hasselmann (1987). Yearly CO_2 emission rates are assumed to be constant for the current year, so Equation (4) is integrated analytically one year at a time.

The uptake of anthropogenic CO_2 by the oceanic GCM matches very closely that of the box-diffusion (BD) model of Oeschger *et al.* (1975), calibrated to give the correct uptake of bomb ^{14}C. As discussed by Bjorkstrom (1986), BD models cannot be made to simultaneously give the correct profile of both prebomb ^{14}C and bomb ^{14}C unless an unrealistically large mixed layer depth (500 m) is assumed. Using a more realistic mixed layer depth requires a larger diffusion coefficient for the transient tracer (bomb ^{14}C) than for prebomb ^{14}C. This discrepancy can be resolved if a larger diffusion coefficient is more appropriate in the main thermocline than in the rest of the ocean, as the transient response would depend most on the diffusion coefficient in the upper ocean. As we are most interested in the transient response to a CO_2 injection, it is encouraging that the oceanic GCM agrees well with the BD model calibrated to bomb ^{14}C. It should be kept in mind, however, that the effective diffusion coefficient for oceanic uptake of a tracer depends on the relationship between input to the ocean surface and outcropping isopycnal surfaces, and can therefore differ from tracer to tracer (or between heat and tracers, as discussed in Harvey, 1986). We can nevertheless expect the input pattern for CO_2 to be closer to that of ^{14}C than to other tracers, as discussed by Emanuel *et al.* (1985).

The oceanic GCM used to deduce $G(t)$ advects carbon by the three-dimensional current field and includes a 7-component chemistry for computing air-sea exchanges, but neglects biological oceanic carbon cycle processes and contains no feedback between temperature and the oceanic CO_2 partial pressure pCO_2 or between climate and the oceanic circulation. The neglect of biological processes affects the simulation of the present-day distribution of oceanic carbon but should have little impact on the magnitude of perturbations superimposed on the present-day distribution.

Feedback between temperature and oceanic pCO_2 is accounted for here as follows: For a given salinity and alkalinity, mixed layer pCO_2 is a function of mixed layer temperature T and total dissolved carbon TC, so that small changes in pCO_2 can be approximated by

$$\mathrm{d}pCO_2 = \left.\frac{\partial pCO_2}{\partial T}\right|_{TC} \Delta T + \left.\frac{\partial pCO_2}{\partial TC}\right|_{T} \Delta TC. \tag{5}$$

The convolution integral (1) accounts for the second term of Equation (5) but neglects the first. We account for temperature feedback on mixed layer pCO_2 by using $(1/pCO_2)\,\partial pCO_2/\partial T = 0.043\ ^\circ C^{-1}$, based on Peng *et al.* (1987), along with

the mixed layer temperature change ΔT as computed by the climate model. Let ΔpCO_{2m} be the perturbation in mixed layer pCO_2 due to temperature changes. This will lead to a perturbation flow of carbon between the mixed layer and atmosphere, not accounted for by the convolution integral, and a perturbation of atmospheric pCO_2, ΔpCO_{2a}, governed by

$$\frac{d\Delta pCO_{2a}}{dt} = \gamma(\Delta pCO_{2m} - \Delta pCO_{2a}). \tag{6}$$

Heimann *et al.* (1986) indicate a coefficient for ocean-air CO_2 exchange of 2.166 kg C day^{-1} m^{-2} atm^{-1}. Using an ice-free global ocean fraction of 0.65 and a factor of 0.469 to convert from atmospheric CO_2 as GT C to ppmv, $\gamma = 0.122$ yr^{-1} if ΔpCO_{2a} and ΔpCO_{2m} are given in ppmv. Equation (6) is integrated analytically one year at a time with constant ΔpCO_{2m}, which is updated at the start of each new year. This leads to a continuously changing atmospheric perturbation ΔpCO_{2a} which is added to the concurrent atmospheric CO_2 concentration computed from the convolution integral.

The neglect of feedback between climate and oceanic circulation is a more serious limitation, but at the moment even the sign of the effect of such feedback on atmospheric CO_2 is unknown. A decrease in the rate of oceanic circulation in the vertical plane would have two competing effects on atmospheric CO_2: a likely reduction in oceanic biological productivity, and a reduction in the rate of upwelling of CO_2-rich deep water. Sarmiento and Toggweiler (1984), Baes and Killough (1986), and Goudriaan (1989) all found that a decrease in the magnitude of oceanic circulation lowered atmospheric pCO_2, while Baes (1982) and Broecker and Takahashi (1985) suggest the opposite. Rather than attempting to compute this feedback, we examine the magnitude of CO_2 emission reductions required to stabilize atmospheric CO_2 at various concentrations assuming no change in oceanic circulation, then use the most rapid natural rates of change of atmospheric CO_2 estimated from ice core data to set limits on the magnitude of the perturbation in ocean-air CO_2 flux that could result from oceanic circulation changes, and examine the extent to which such perturbations could be counteracted by a further reduction of CO_2 emissions or other strategies.

Finally, it should be noted that the unperturbed carbon cycle is assumed to be in steady state. This is undoubtedly only an approximation, as atmospheric CO_2 seems to have increased from 250 to 300 ppmv between A.D. 1250 and 1550, then decreased to 260 ppmv by 1650 before rising to its immediately pre-industrial level of 280–285 ppmv (Gammon *et al.*, 1985). These perturbations and rates of change are nevertheless smaller than in recent decades or than projected for the future.

Terrestrial Biosphere

Although the size of the terrestrial biosphere (about 2000 GT C, including soil C) is small compared to the potentially exploitable fossil fuel resource (5000–14 000

GT C), feedbacks involving the terrestrial biosphere could be of importance for scenarios of decreasing fossil fuel CO_2 emissions. A 6-box, globally aggregated terrestrial biosphere model is therefore coupled to the climate-carbon cycle model. This model is illustrated in Figure 1, and corresponds to model version 8 of Harvey (1989c), where a fuller description and sensitivity analysis may be found. The model contains boxes representing ground vegetation, non-woody tree parts, woody tree parts, detritus, and two soil reservoirs having turnover times of 75 and 500 yrs.

The model includes stimulation of NP (net photosynthesis) or NPP (net primary productivity, equal to NP minus respiration by woody tree parts) by enhanced atmospheric CO_2 using the β factor introduced by Bacastow and Keeling (1973), whereby

$$N = N_0(1 + \beta \ln(CO_2(t)/CO_2(0))), \tag{7}$$

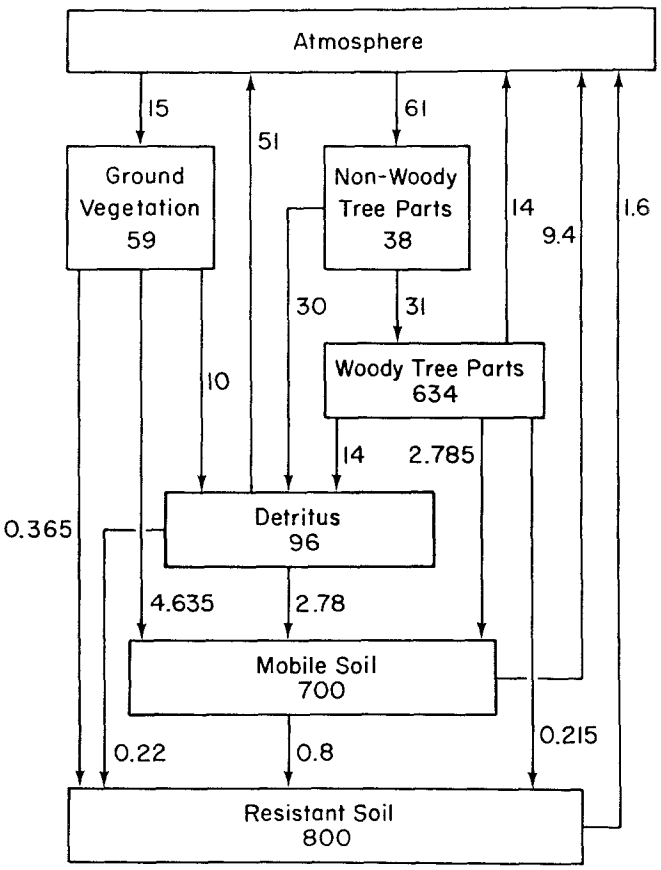

Fig. 1. The terrestrial biosphere model used here. Numbers in boxes correspond to the original reservoir sizes (GT C) assumed for 1770, when the simulations begin. Numbers next to arrows indicate the initial fluxes (GT C yr^{-1}).

where N_0 and $CO_2(0)$ are the initial NPP (or NP) and CO_2 concentration. Unlike Bacastow and Keeling (1973), NPP is not assumed to be proportional to photosynthetic biomass but instead varies logistically with biomass. The model also allows the rates of a number of processes to vary with temperature using a Q_{10} formulation, such that

$$M = M_0(Q_{10})^{(T - T_0)/10}, \tag{8}$$

where M_0 is the initial rate of process M and T_0 is the initial temperature. As seen from Equation (8), Q_{10} is the factor by which a given process increases for each 10 °C temperature increase. A Q_{10} of 1.53 is used for NP of non-woody tree parts and of 1.4 for NPP of ground vegetation, while a Q_{10} of 2.0 is used for respiration of woody tree parts, detritus and soil, as well as for the coefficient for carbon transfer from detritus to soil and from the rapidly to slowly overturning soil reservoirs. The transfer coefficient from non-woody to woody tree parts, representing translocation, also increases with a Q_{10} of 2.0. The separate Q_{10}'s for NP and respiration give a tree NPP having an effective Q_{10} of about 1.4. Justification for these feedbacks may be found in Harvey (1989c).

Increases in both temperature and CO_2 lead to an increase of NPP and NP. In the case of ground vegetation, the equilibrium biomass is assumed to increase by the same factor as the enhancement of NPP, whereas in the case of non-woody tree parts, the equilibrium biomass is assumed to increase by the same factor as the increase in NP due to increased CO_2 alone. This is because a temperature increase also leads to an increase of translocation from non-woody to woody tree parts. The assumptions utilized here cause the ratio of translocation: NP to increase with a Q_{10} of about 1.4, which is consistent with data cited in Harvey (1989c).

Land use changes during the past several hundred years have resulted in a significant flux of CO_2 to the atmosphere, with a corresponding removal of carbon from the terrestrial biosphere. The net flux to the atmosphere from land use changes is a residual resulting from large gross fluxes associated with deforestation and biomass burning, partly compensated by regrowth after disturbed areas have been abandoned. Emanuel *et al.* (1984) incorporated the effect of such disturbances and regrowth in a terrestrial biosphere model similar to the one used here; their formulation allows for partial recovery of living biomass following removal of vegetation, as well as for changes in the detrital and soil reservoirs. This formulation is not adopted here because we wish to explicitly specify the gross fluxes to and from the atmosphere resulting from land use changes (see Section 3.2). Having specified the gross fluxes due to land use changes, the resultant net flux is removed from all 6 biosphere boxes in proportion to their initial masses. The parameters controlling the asymptotic biomasses are also adjusted so that the net removal of biomass due to land use changes induces no compensating adjustments in the biosphere model. The response of the terrestrial biosphere model to CO_2 and temperature increases therefore represents the response of the 'undisturbed' biosphere.

The model does not include potentially important carbon fluxes associated with

forest dieback during the transient response to rapid climatic warming, whereby forests at the equatorward margins of their range die faster than other species can migrate to replace them (Solomon, 1986).

Miscellaneous CO_2 Sinks

For some reconstructions of historical CO_2 emissions, an additional sink is required in order to match the observed CO_2 increase. The accumulation of carbon in coastal sediments might have increased by 0.6 to 1.6 GT yr^{-1} in recent decades, with further sinks of up to 0.2 GT C yr^{-1} due to enhanced dissolution of marine carbonates (Baes *et al.*, 1985), and up to 0.2 GT yr^{-1} due to an increase in the accumulation of carbon in lake and reservoir sediments (Mulholland and Elwood, 1982). The total additional sink in 1980 could therefore be up to 1.8 GT C yr^{-1}, of which about one third could be induced by nitrogen fertilization and hence be independent of the CO_2 increase.

We assume the existence of a miscellaneous sink S in most experiments, where S varies according to

$$S = \begin{cases} S_{1980}(t-1770)^2/210^2 & t \leqslant 1980 \\ S_{1980}(f(C(t)-C(1770)/(C(1980)-C(1770)+(1-f)) & t > 1980 \end{cases}, \quad (9)$$

where S_{1980} is the assumed 1980 value of the sink, t is time in years since 1770, C is atmospheric CO_2 concentration, and $f = 2/3$ is the fraction of the 1980 sink assumed to be directly dependent on the CO_2 increase since 1770, and which continues to grow in proportion to the CO_2 buildup. S_{1980} is $\leqslant 1.8$ Gt C yr^{-1}.

3. CO_2 Emission and Trace Gas Scenarios

3.1. *Fossil Fuel CO_2*

Fossil fuel and cement-derived CO_2 emissions for 1860–1984 are taken from Rotty (1980, 1987) and are assumed to be zero prior to 1860. Given 1984 global CO_2 emissions for solids, liquids and gases from Rotty (1987) and UN data for the 1984 primary consumption of these fuels, we compute mean CO_2 emission factors of 13.56 Mt C/EJ for gases, 21.14 Mt C/EJ for liquids, and 24.95 Mt C/EJ for solids. With these emission factors, the 1985 and 1986 fossil fuel CO_2 emission is estimated as 5.28 and 5.38 GT C using the UN (1988) compilation of global energy use in 1985 and 1986. The 1984 cement-derived emission of 0.13 GT C is added to these estimates.

Fossil fuel emissions are assumed to increase at a rate γ_1 of either 0% or 1% yr^{-1} from 1986 until either 2000 or 2020, at which point it is assumed that deliberate global actions are taken to begin a transition to a rate of decrease γ_2 of fossil fuel emissions of either 1% or 2% yr^{-1}. The time when the rate of increase of CO_2 emissions begins to decrease shall be referred to as the Action Initiation Time (AIT),

following Perry *et al.* (1982). The transition from γ_1 to γ_2 is generally assumed to require $5(\gamma_1 + \gamma_2)$ years, so that, for example, 10 years are required for the transition form a 1% yr^{-1} increase in fossil fuel CO_2 emissions to a 1% yr^{-1} decrease. Cement-derived emissions are assumed to grow to twice their 1984 value by 2100, then remain constant. If and when total industrial emissions decrease to the CO_2 uptake by the oceans and other sinks, subsequent emissions are set equal to the total sink strength and hence decrease at the same rate as the decrease in total sink strength.

3.2. *Emissions Due to Land Use Changes*

Current and Future Emissions

Houghton *et al.* (1983; hereafter H83) estimated the 1980 CO_2 emission from global land use changes to be 0.5–4.5 GT C. Houghton *et al.* (1985; 1987; hereafter H85 and H87) recomputed the 1980 flux with revised data and estimated a likely range of 1.0–2.6 GT C, with all but 0.1 GT C being from the tropics. Detwiler and Hall (1988) estimated the 1980 emission from the tropics to be 0.4–1.6 GT C. Detwiler and Hall (1988), H85, and H87 all used forest biomass data of Brown and Lugo (1982, 1984) in their calculations. Based on an exchange of letters in *Science* (volume 241, pages 1736–1739) it appears that most of the difference between H85 and H87 on the one hand, and Detwiler and Hall (1988) on the other, is due to an incorrect use of the Brown and Lugo biomass data on the part of H85 and H87. However, Fearnside (1985, 1986) argues that above-ground biomass in the Brazilian Amazon is about twice that indicated by Brown and Lugo (1982, 1984), so a net land use flux in 1980 of 2.5 GT C cannot be ruled out. In this paper we shall consider cases in which the net emission in 1980 due to land use changes is assumed to be 1.0 and 2.5 GT.

The net emission due to land use changes is a residual of much larger gross fluxes of opposite sign. Among the above-cited papers, only H83 provide data on calculated gross emissions. For assumptions leading to an estimated 1980 net emission of 2.6 GT C, the gross emission due to harvesting of forests, decay of wood products, and expansion of cropland and pastureland is 4.6 GT C. From the point of view of short term management of atmospheric CO_2, it is the gross and not the net emission which is important. Much of the gross emission is compensated by regrowth of forests on previously disturbed land. A given fractional reduction in the rate of deforestation will cause a corresponding decrease in the gross emission, but the sink due to regrowth of forests will decrease only over a period of 3–5 decades, depending on how rapidly forests recover from previous deforestation. Since the gross flux is substantially greater than the net flux, the potential impact on CO_2 emissions of reducing the rate of global deforestation is greater than might be inferred based on the net emission, at least initially.

To illustrate the potential contribution to stabilizing atmospheric CO_2 of reducing

the rate of global deforestation, gross fluxes consistent with the assumed 1980 net fluxes of 1.0 and 2.5 GT C are needed. Differences between the lower and upper emission estimates in H85 or H87, and between estimates published in 1983 and later, are a result of differences in the assumed carbon stocks of undisturbed forests, differences in the assumed rates of deforestation, differences in the assumed loss of soil carbon following conversion of forests to cropland, and differences in accounting procedures. The upper emission estimate of 2.6 GT C for 1980 given in H85 and H87 corresponds to carbon stocks similar to those used in computing the gross emissions given in H83, but assumes larger rates of deforestation and smaller soil carbon losses. We therefore use the same gross fluxes, modified slightly, for a net emission of 2.5 GT C yr^{-1} (Table II). To estimate gross fluxes associated with a net emission of 1.0 GT C yr^{-1}, we make use of data given in Table IV of H85, which shows the separate contribution of uncertainty in carbon stocks and in deforestation rates to net emission in different regions. We also assume that the uncertainty in the estimated emission due to conversion of shifting agriculture to permanent agriculture derives equally from uncertainty in carbon stocks and in rates of land use change. Going from high stocks and high deforestation rates to low stocks and high deforestation rates reduces the emission from 2.5 to 1.5 GT C; the difference of 1 GT C is partitioned among the emission terms due to forest harvest and expansion of cropland and pastureland in proportion to their sizes, as given in column 2 of Table II. The remaining 0.5 GT C reduction, due to lower rates of deforestation, is partitioned among the first 4 terms of Table II, giving the resultant gross fluxes shown in the last column.

Rates of deforestation in Brazil increased substantially between 1980 and 1987, with 80 000 km^2 deforested in 1987 in Brazil alone, compared to 100 000 km^2 deforested worldwide in 1980 (Salati, personal communication, 1988). Here, the

TABLE II: Gross fluxes in 1980 due to land use changes as estimated by Houghton *et al.* (1983) for a case in which estimated net emission is 2.6 GT C, as well as gross fluxes assumed here to be associated with net emissions of 1.0 and 2.5 GT C in 1980. Gross emissions due to forest harvesting and agricultural expansion are assumed to increase a further 50% between 1980 and 1987

	Houghton *et al.* (1983)	1980 Net Emission (GT C)	
		2.5	1.0
Forest harvest	2.49	2.40	1.15
Forest regrowth	−1.86	−1.87	−1.17
Expansion of			
cropland	1.58	1.57	0.75
pastureland	0.24	0.24	0.11
Decay of forest products	0.27	0.27	0.27
Abandonment and afforestation	−0.11	−0.11	−0.11
Emission to 1980:		205	123

gross emissions associated with agricultural expansion and forest harvesting are assumed to increase by 50% between 1980 and 1987. This gives gross emissions in 1985 of 2.7 and 5.7 GT C for the 1980 low and high emission cases, respectively. By comparison, Andreae *et al.* (1988) estimated the gross emission due to biomass burning worldwide in 1985 to be 2–4 GT C. This rough estimate does not include delayed releases due to decomposition of unburnt detritus or oxidation of soil carbon, and therefore might be compatible with the range of 1985 emissions assumed here.

As deforestation rates and associated land abandonment increase, the CO_2 sink due to regrowth of forests will increase. It is assumed here that forests require 50 yrs (based on H83) to regrow to their new equilibrium biomass (which is less than their original biomass), and that the CO_2 uptake due to forest regrowth after 1980 increases at a rate such that it would reach 1.5 times the 1980 rate of uptake by 2030. This only crudely mimics what is likely to happen in reality.

For future land use emissions, high and low deforestation scenarios are considered. In both cases, gross emissions are held constant after 1987 until some time t_1, at which point a uniform reduction in the CO_2 emission due to harvesting of forests to 75% of the 1980 value occurs by year t_2, while the emissions due to expansion of croplands and pasturelands decrease uniformly to 50% and 0%, respectively, of their 1980 values by year t_2. After t_2, forest harvest emissions are constant but emissions due to agricultural expansion continue to decrease to zero by 2100[2]. The CO_2 released by decay of wood products is assumed to be constant at all times after 1980. The CO_2 sink due to regrowth of forests after harvesting is assumed to increase linearly over a 50 yr period from its value at time t_2 to a value equal to the emission due to harvesting of forests and decay of wood products. This assumes that future harvesting of forests involves secondary rather than virgin forest, and that secondary forests keep growing back to the same biomass 50 yrs after harvest (these assumptions clearly imply careful forest management). For the high deforestation scenario, t_1 is 2035 and t_2 is 2070, while for the low deforestation scenario these years are 1990 and 2000, respectively. Table III summarizes the gross emissions in 1980, 1987, t_1, t_2, and 2100.

Figure 2 shows the variation of gross land use emission, CO_2 uptake by regrowth, and net emission between 1980 and 2100 for the low and high deforestation scenarios, assuming net emissions in 1980 of 1.0 and 2.5 GT C. Note that the fractional increase of net emission between 1980–1987 is substantially larger than the 50% increase of gross emissions assumed for this period. Also note that with constant gross emissions between 1987–2035, the net emission gradually decreases as land abandoned prior to 1987 becomes fully recovered but is replaced with larger areas undergoing recovery which were abandoned after 1987. For the low

[2] See Goldemberg *et al.* (1988) for a discussion of how energy, agricultural, and timber needs of a growing world population could be simultaneously satisfied on a sustainable basis. The land use scenario used here implicitly assumes that global population stabilizes by 2100.

TABLE III: Gross fluxes due to land use changes at various times in the future for the high and low deforestation scenarios. The same relative changes in fluxes are assumed to occur for both scenarios, but at different times

Flux		Year			
	High deforestation:	1980	1987–2035	2070	2100
	Low deforestation:	1980	1987–1990	2000	2100
		1980 net flux of 1 GT C			
Cropland expansion		0.75	1.13	0.38	0.00
Pastureland expansion		0.11	0.17	0.00	0.00
Forest harvest		1.15	1.73	0.86	0.86
Forest product decay		0.27	0.27	0.27	0.27
		1980 net flux of 2.5 GT C			
Cropland expansion		1.57	2.36	0.79	0.00
Pastureland expansion		0.24	0.32	0.00	0.00
Forest harvest		2.40	3.20	1.80	1.80
Forest product decay		0.27	0.27	0.27	0.27

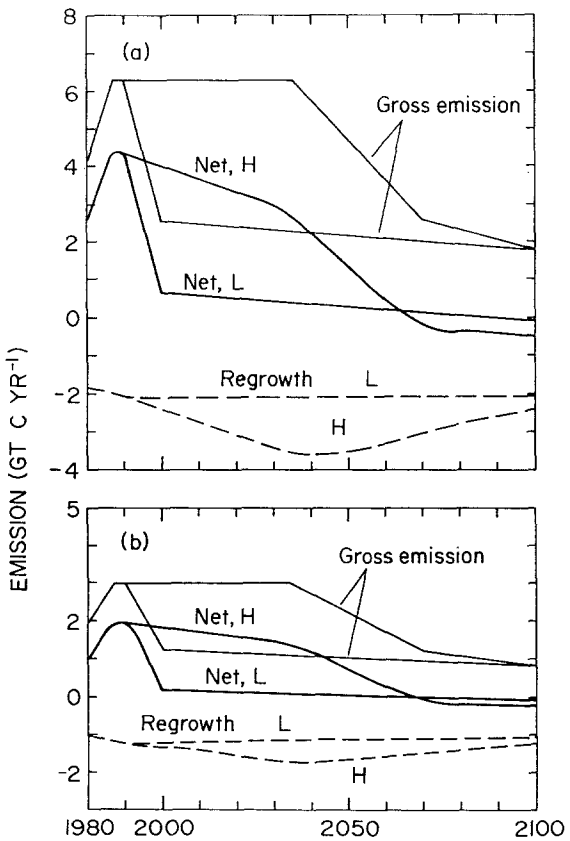

Fig. 2. Variation of gross and net carbon emission between 1980 and 2100 due to land use changes for net emissions in 1980 of (a) 2,5 GT C and (b) 1.0 GT C. H = high deforestation scenario, L = low deforestation scenario.

deforestation scenario, net emission drops to near zero by the year 2000 as the gross emission, although still large, is comparable to the regrowth sink.

The scenarios shown in Figure 2 are intended for illustrative purposes only. An important characteristic of these scenarios is that cutting the rate of deforestation in half is sufficient to reduce the net CO_2 flux to the atmosphere due to land use changes to about zero. Charles Hall kindly consented to run the land use model of Detwiler and Hall (1988) for a scenario in which the rate of deforestation decreased linearly from its 1980 value to zero over a period of 25 yrs. For both open and closed forest cases, the net flux due to deforestation decreased to zero by the time the rate of deforestation had decreased to half its 1980 value. This is in agreement with the behavior of the net flux shown in Figure 2, and is a consequence of the gross emission being about twice the net emission.

Past Emissions

Estimates of emissions prior to 1980 were derived from the emission curve for 1860–1980 of Figure 8 of H83. Their values are based on their 1980 flux estimate of 2.6 GT C. We uniformly scale this curve to match our upper limiting 1980 net flux of 2.5 GT C.

As discussed in Houghton (1986), differences in the timing of past land use changes can lead to large differences in the estimated net CO_2 flux to the atmosphere in 1980, even when the cumulative areas involved are the same. In H83, the integrated emission from 1860–1980 varies between only 180–185 GT C as the 1980 flux ranges from 2.6 to 4.7 GT C for different scenarios of historical land use changes, but assuming the same initial carbon stocks. It is therefore not appropriate to uniformly scale the H83 emission curve corresponding to a 1980 emission of 2.6 GT C to get a curve corresponding to a 1980 emission of 1.0 GT C (our lower limiting case).

In the present study, the uncertainty in the 1980 flux (1.0–2.5 GT C) is partly due to uncertainty in undisturbed carbon stocks. This uncertainty would apply to earlier deforestation as well. Here, for the scenario having a 1980 emission of 1.0 GT C, we simply reduce the pre-1920 fluxes by 30%, and reduce post-1920 fluxes by an amount increasing linearly to 60% in 1980. The emission in 1770, when the model begins, is assumed to be half the emission in 1860, and to increase linearly to the 1860 value. Cumulative emissions to 1980 are 123 GT C and 205 GT C for the low and high emission scenarios, respectively (Table II).

3.3. *Non-CO_2 Greenhouse Gases*

Atmospheric concentrations of the chlorofluorocarbons CFC11 and CFC12 are specified up to 1986 from Wigley (1986), and computed thereafter using Wigley's (1988) two box model, which requires as input the global rate of production of rapidly and slowly released CFC's. Following Wigley (1988), the production of

rapidly released CFC's as a fraction of total CFC production is assumed to decay exponentially with time. We consider scenarios in which total CFC production decreases to 50% of the 1986 production by 1998, as required by the Montreal Protocol on Ozone Depleting Substances (UNEP, 1987), and is then held constant, or decreases to zero by 2003.

Scenarios of past and future concentration of CH_4 and N_2O are taken from Wigley (1986) but are modified to allow for restrictions in their production once CO_2 emissions begin to decrease. Perturbations in the net surface-troposphere radiative heating from these gases as well as CFC's and CO_2 are computed using formulae of Wigley (1986), which were derived from detailed radiative transfer models. As well, it is assumed that an increase of tropospheric ozone is initially correlated with the buildup of CH_4 and contributes a further radiative heating of 1/3 that due to CH_4 alone (see Ramanathan *et al.*, 1987 and Dickinson and Cicerone, 1986). Base case trace gas scenarios and radiative forcings are summarized in Table IV.

A substantial fraction of the increase of N_2O might be due to combustion of fossil fuels (Weiss, 1981) but the atmospheric lifetime of N_2O is about 120 yrs (Ramanathan *et al.*, 1987), so it is assumed that N_2O remains constant once fossil fuel CO_2 emissions begin to decrease. The relative importance of fossil fuel use and non-fossil fuel sources to anthropogenic CH_4 is uncertain; it is assumed here that half of the CH_4 buildup is unrelated to fossil fuel use, and the other half is associated with fossil fuel use. The atmospheric lifetime of CH_4 is about 7 yrs (Wang *et al.*, 1986), so it is assumed that the portion of the excess CH_4 attributed to fossil fuel use decreases in proportion to the decrease in fossil fuel CO_2 emissions, but that the other portion remains constant once CO_2 emissions decrease.

TABLE IV: Scenarios for CH_4, N_2O, and radiatively effective CFC concentration C (ppbv), and radiative forcing Q ($W\,m^{-2}$) for CO_2, CH_4, N_2O, and CFC's. CH_4 and N_2O increase until fossil fuel CO_2 emissions begin to decrease. The C_0 are initial concentrations

Trace gas concentration		
CH_4	1765–1951:	$C = 790 + 0.0101(y - 1765)^2$
	>1951:	$C = 1643 + 14.81(y - 1985)$
N_2O	1900–1975:	$C = 280 + 0.000042(y - 1900)^3$
	>1975:	$C = 258.5 + 0.0068(y - 1899.1)^2$
CFC's	1950–1986:	$C_{11} = 0.18(y - 1950)^2$
		$C_{12} = 1.7\ C_{11}$
	⩾1986:	computed from two-box model
Radiative forcing		
CO_2		$Q = 4.2\ \ln(C/C_0)/\ln(2)$
CH_4		$Q = 0.0398\ (\sqrt{C} - \sqrt{C_0})$
N_2O		$Q = 0.105\ (\sqrt{C} - \sqrt{C_0})$
CFC		$Q = 1.32\ (0.00027\ C_{11} + 0.00031\ C_{12})$

Finally, since the increase of tropospheric O_3 is related to fossil fuel use and any dependence on CH_4 occurs only in the presence of NO_x (Ramanathan *et al.*, 1987), it is assumed that total tropospheric O_3 forcing decreases in proportion to fossil fuel CO_2 emissions once these emissions begin to decrease.

4. Results

4.1. *Temperature and CO_2 Simulation to 1984*

We first determine parameter values under which the coupled climate-carbon cycle model can simulate both the observed atmospheric temperature increase from 1860 to the present and the inferred CO_2 increase from pre-industrial levels to the 1958 and 1984 values. The pre-industrial CO_2 concentration appears to have been 280–285 ppmv (Oeschger and Stauffer, 1986), and had risen to 315 ppmv by 1958 and 344 ppmv by 1984 (Solomon *et al.*, 1985). Global mean atmospheric temperature increased by 0.5 ± 0.2 °C during the past 120 yrs (Jones *et al.*, 1986). As shown by Wigley (1987), if this temperature increase were caused by the buildup of greenhouse gases, it implies that $\Delta T_{2x} = 1.2$–2.0 °C if there were no counteracting cooling effects. It is possible that industrial SO_2 emissions have served to partially counteract the greenhouse gas increase, so that a ΔT_{2x} as large as 5.0 °C could be compatible with observations (Wigley, 1989).

Figure 3a shows the computed atmospheric temperature variation from 1750 to 1987 for $\Delta T_{2x} = 2.0$ °C and 4.0 °C, along with the globally averaged surface air temperature variation from 1880 to 1987 as determined by Hansen and Lebedeff (1988). The computed temperature variation matches the long term warming since 1880. The shorter term oscillations superimposed on the observed long term warming could have been caused by changes in solar luminosity and volcanic activity (Gilliland and Schneider, 1984) or by changes in deep ocean circulation (Gaffin *et al.*, 1986; Wigley and Raper, 1987).

Table V gives simulated atmospheric CO_2 concentrations in 1958 and 1984, assuming CO_2 emissions from land use changes which grow to 1.0 or 2.5 GT C yr^{-1} by 1980. Also given in Table V are the cumulative fluxes to the atmosphere up to 1984 due to land use changes and from temperature- and CO_2-biosphere feedback. Even the smaller land use-induced emission gives too large an atmospheric CO_2 buildup if $\beta = 0.4$. If the biosphere and land use changes are omitted altogether, CO_2 concentrations are 5–7 ppmv below those observed in 1958 and 1984 (Table V). With land use emissions, the CO_2 variation can be made to fit observations by either using $\beta > 0$, altering the oceanic τ_i (Equation 3) to give a faster rate of CO_2 uptake, or assuming the existence of additional CO_2 sinks. Table V shows values of β, the additional 1980 carbon sink, S_{1980}, the factor f by which the τ_i need to be multiplied, or combinations thereof, which give close to the observed 1958 and 1984 CO_2 concentrations. Oceanic temperature-pCO_2 feedback con-

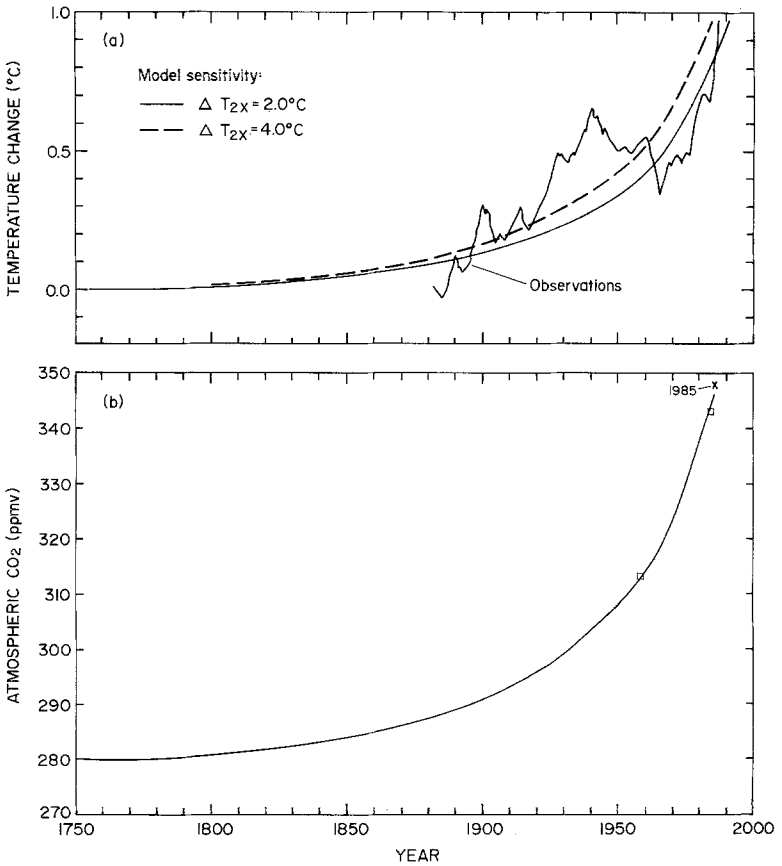

Fig. 3. (a) Model-computed atmospheric temperature variation, 1750–1987, for a $2 \times CO_2$ equilibrium sensitivity of 2.0 °C and 4.0 °C, and observed surface air temperature variation 1880–1987 from Hansen and Lebedeff (1988). (b) Model-computed atmospheric CO_2 concentration, 1750–1984, and observed atmospheric CO_2 concentration, 1958–1984.

tributes 3–6 ppmv to the computed atmospheric CO_2 concentration in 1958 and 7–11 ppmv 1984.

Previous workers have found $\beta = 0.2$–0.6 necessary to simulate the correct CO_2 buildup (Bacastow and Keeling, 1973; Gifford, 1980; Goudriaan and Ketner, 1984), in the absence of additional sinks. For a 1980 land use emission of 1.0 GT C, $\beta = 0.6$ is required if there is no additional sink, or an additional sink of 1.5 GT C is required if $\beta = 0.0$. A β of 0.6 is probably unreasonably high, as β's measured under ideal growing conditions (adequate water, light, and nutrients) are 0.5–0.75 for a variety of plants (Gates, 1985), and decrease as atmospheric CO_2 increases. Further evidence against a β this large is that the net cumulative biospheric emission for this case is only 31 GT C (Table V), compared to a cumulative emission to 1980 of 90–150 GT C estimated by Siegenthaler and Oeschger (1987)

TABLE V: Atmospheric CO_2 concentrations in 1958 and 1984 for various combinations of 1980 CO_2 emissions due to land use changes (L_{1980}), β factor, 1980 miscellaneous CO_2 sink (S_{1980}), and multiplication factor f for the oceanic time constants for CO_2 uptake. Also given are cumulative emissions to 1984 due to land use changes and temperature and CO_2 feedback on the terrestrial biosphere. Units are GT C yr^{-1} for L_{1980} and S_{1980}, ppmv for concentrations, and GT C for cumulative emissions

				Concentration		Total emission	
L_{1980}	β	S_{1980}	f	1958	1984	Land use	Feedback
0.0	0.0	0.0	1.0	305.6	341.6	0	0
	0.0	0.0	1.0	331.4	374.3	128	1
1.0	0.6	0.0	1.0	314.6	345.3	128	−97
	0.4	0.5	1.0	313.6	345.2	128	−62
	0.2	1.0	1.0	312.1	344.9	128	−29
	0.0	1.5	1.0	309.9	343.5	128	1
	0.4	0.0	0.5	313.4	342.8	128	−61
	0.0	0.0	1.0	346.1	401.3	218	−2
2.5	0.4	1.8	1.0	311.0	345.6	218	−58
	0.4	1.2	0.5	312.3	344.6	218	−59

Results are given for $\Delta T_{2X} = 2.0$ °C, and assume a pre-industrial CO_2 concentration of 280 ppmv.

by deconvolution of ice core CO_2 and $^{13}\delta$ records.[3] A β of 0.4 is therefore used here as an upper limit in simulating past and future CO_2 variations. Figure 3b shows the computed CO_2 variation for this case.

If we assume that $\beta = 0.4$, then for a 1980 land use emission of 2.5 GT C we must also assume our estimated upper limit of 1.8 GT C yr^{-1} for additional carbon sinks; we therefore cannot consider a smaller β for this scenario unless the τ_i are reduced. Furthermore, the cumulative biospheric emission for the upper limiting land use scenario with $\beta = 0.4$ is 160 GT C, and assuming a smaller β would put it further outside the range of 90–150 GT C estimated by Siegenthaler and Oeschger (1987). Thus, assuming the upper limit for land use emissions – 2.5 GT C in 1980 – requires assuming the upper limits for both β and additional sinks. Reducing the oceanic τ_i in half has comparatively little effect on this result.

The modelled atmospheric CO_2 increases by 3.0 or 3.2 GT C in 1980 for the low and high land use emission assumptions, respectively, compared to an observed increase of 3.5 GT C (Heimann *et al.*, 1986). By 1987 the model-computed increase had risen to 3.8 or 4.6 GT C yr^{-1}, compared to an observed increase between January 1987 and January 1988 of 4.8 GT C based on the average of Mauna Loa and South Pole data (Keeling, pers. commun., 1988).[4]

Finally, if we assume a land use emission of 1.0 GT C in 1980, the biosphere switches from a net source to a net sink of carbon between 1960 and 1980 for β

[3] Siegenthaler and Oeschger's (1987) results were obtained with use of a carbon cycle model and are therefore model-dependent.

[4] Part of the recent acceleration of CO_2 buildup may reflect a short term oscillation in ocean-atmosphere or biosphere-atmosphere CO_2 fluxes.

values of 0.4 or 0.6, but does not become a net sink for a β of 0.2, or for a 1980 land use emission of 2.5 GT C. Some reconstructions of past net biospheric emissions indicate that the biosphere became a net sink after 1960, depending on the model or data used (Peng and Freyer, 1986; Siegenthaler and Oeschger, 1987). For most cases in which the model biosphere becomes a net sink after 1960, it becomes a net source again in the early 1980's due to increased deforestation.

4.2. *Business as Usual Scenario*

As a reference case against which the effect of CO_2 emission and other greenhouse gas control strategies can be compared, we consider a 'business as usual' scenario in which fossil fuel emissions grow at a rate $\gamma_1 = 1.8\%\ \text{yr}^{-1}$ until 2075, followed by a transition to an emission decrease γ_2 of $1\%\ \text{yr}^{-1}$ after 2125. We also assume that CH_4 and N_2O increase until 2075 according to the formulae given in Table IV (with a concurrent increase of tropospheric O_3), that CFC production remains constant at 0.5 the 1986 production after 1998, and that the high deforestation scenario (Table III) occurs. The fossil fuel CO_2 emission for this scenario corresponds roughly with the 75th percentile of Edmonds *et al.*, (1986) up to 2075 (i.e. 25% of their scenarios gave higher emissions), and is comparable to that of the 'low' IIASA scenario (Hafele, 1981) up to 2020 (when their projection ended). The total fossil fuel emission to the year 2300 is 5400 GT C.

Table VI gives peak temperature increases above the simulated 1980 temperature, peak rates of temperature change, peak atmospheric CO_2 concentrations, the contribution of temperature-pCO_2 feedback to peak atmospheric CO_2, and cumu-

TABLE VI: Business as usual scenario: Peak atmospheric temperature increase above the simulated 1980 temperature ($\Delta T_{\max}$, °C), peak rates of temperature change (dT/dt, °C decade^{-1}), peak atmospheric CO_2 concentration (CO_2, ppmv), contribution of temperature-pCO_2 feedback to peak atmospheric CO_2 (ΔCO_2, ppmv), and cumulative emissions (GT C) to 2300 due to land use changes and biosphere feedback. Results are given for alternative ΔT_{2x}, L_{1980}, β, S_{1980}, and ocean CO_2 time constant multiplication factor f.

Case					Results					
									Emission	
ΔT_{2x}	L_{1980}	β	S_{1980}	f	$\Delta T_{\max}$	dT/dt	CO_2	ΔCO_2	Land	$\beta - T$
2.0	1.0	0.4	0.5	1.0	4.4	0.32	1127	104	207	−690
		0.0	1.5	1.0	4.1	0.33	989	93	207	78
		0.4	0.0	0.5	4.3	0.32	1114	102	207	−684
	2.5	0.4	1.8	1.0	3.8	0.33	875	78	407	−527
		0.4	1.2	0.5	3.8	0.32	881	79	407	−531
4.0	1.0	0.4	0.5	1.0	6.9	0.42	1177	165	207	−669
	2.5	0.4	1.8	1.0	5.9	0.38	898	113	407	−545

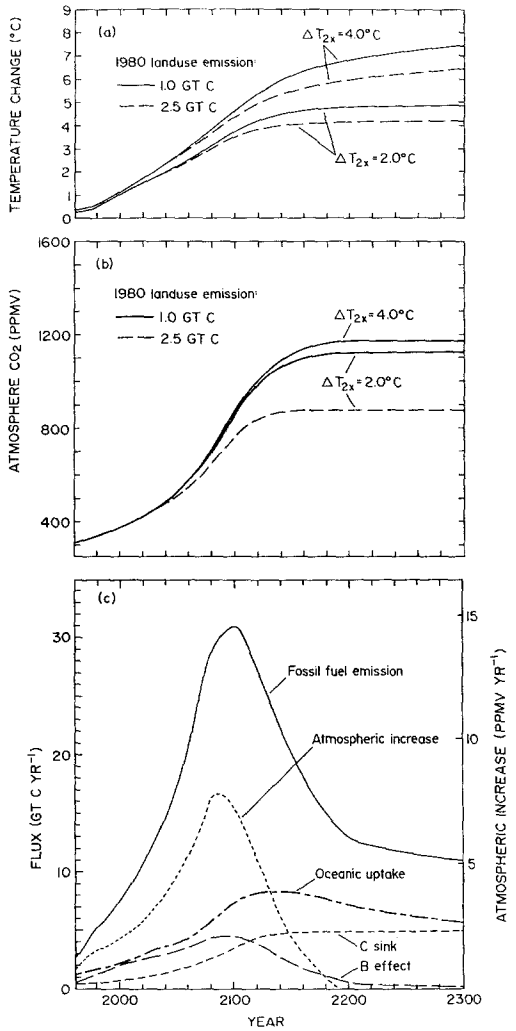

Fig. 4. Variation of atmospheric temperature (a) and CO_2 concentration (b) between 1950 and 2300 for the business-as-usual scenario with alternative land use emissions in 1980 and climate sensitivities (ΔT_{2x}). (c) Variation of fossil fuel emission, atmospheric CO_2 increase, and uptake by CO_2 sinks for the business-as-usual scenario with a 1980 land use emission of 1 GT C, $\beta = 0.4$, and $S_{1980} = 0.5$ GT C yr^{-1}.

lative emissions to the year 2300 due to land use changes and biospheric feedback. Results are given for ΔT_{2x} = 2.0 °C and 4.0 °C and for 1980 land use emissions of 1.0 and 2.5 GT C.[5] Figure 4 gives the variation of temperature and CO_2 for both

[5] Higher model temperature sensitivity gives a larger peak CO_2 concentration because the temperature-induced increase of oceanic pCO_2 is larger, but the increase of atmospheric CO_2 is smaller than the increase in the perturbation of oceanic pCO_2 in going from low to high model sensitivity. This is because fossil fuel emissions are assumed here to decrease until they become equal to the net of all sinks. A larger ΔT_{2x} causes a smaller oceanic sink, so that fossil fuel emissions are reduced further, which partly compensates for the larger oceanic pCO_2 perturbation due to warming.

1980 land use emissions, as well as the variation of various carbon fluxes for the case having a 1980 land use emission of 1.0 GT C and $\beta = 0.4$. Global mean temperature increases beyond the 1980 value by 3.8 to 6.9 °C, and maximum rates of warming of 0.32 to 0.46 °C decade^{-1} occur; absolute increases and rates of warming could be 2–3 times higher at mid to high latitudes. The model had not reached equilibrium by 2300 for the high sensitivity cases, so that greater warming would have occurred if the simulation had been extended.

Table VII compares the maximum radiative heating perturbation for each gas for this and other scenarios, as well the peak total radiative heating. Since the maximum heating for different gases does not occur at the same time, the sum of the individual terms in Table VII is greater than the maximum total heating. Also given, for comparison, is the perturbation in radiative heating due to each gas in 1980 and the increase in peak heating above the 1980 value. In 1980, non-CO_2 trace gases contributed about 40% of the total heating, whereas for the business-as-usual scenario considered here their contribution to the peak heating is about 20%.

Balancing land use emissions by assuming $\beta > 0$, $S_{1980} > 0$, or $f < 1$ has comparatively little effect on maximum temperatures or rates of warming, as does the mag-

TABLE VII: Peak concentrations (ppbv except ppmv for CO_2), peak radiative forcings (W m^{-2}) due to individual trace gases, and total peak radiative forcing, for selected scenarios. Also given is the contribution of each gas to the 1980 radiative forcing

	Concentrations				
			Gas		
Scenario	CO_2	CH_4	N_2O	CFC11	CFC12
1980 Values:	339	1569	303	0.162	0.275
Business as usual:	1122	2976	469	0.570	1.226
+1% yr^{-1} to 2020:	447	2199	364	0.335	0.571
Constant to 2020:	406	2146	356	0.335	0.571
Constant to 2000:	392	1850	326	0.335	0.571
Immediate action:	373	1717	315	0.335	0.571

	Radiative forcings						
				Gas			
Scenario	CO_2	CH_4	N_2O	CFC's	$T-O_3$	Total	Change since 1980
1980 Values:	1.17	0.46	0.07	0.17	0.14	2.01	0.0
Business as usual:	8.40	1.05	0.52	0.71	0.35	10.57	8.60
+1% yr^{-1} to 2020:	2.83	0.75	0.25	0.35	0.25	3.96	1.95
Constant to 2020:	2.25	0.73	0.23	0.35	0.24	3.46	1.45
Constant to 2000:	2.04	0.59	0.14	0.35	0.20	3.01	1.00
Immediate action:	1.74	0.53	0.11	0.35	0.18	2.75	0.74

Results for scenarios 2–4 are for low trace gas buildup and low rates of deforestation. For all scenarios, $\beta = 0.4$, $S_{1980} = 0.5$ GT C yr^{-1}, and land use emission in 1980 is 1.0 GT C.

nitude of the 1980 land use flux which needs to be balanced. Assuming a larger 1980 land use emission results in smaller projected CO_2 concentrations and temperatures, because a larger current emission requires a larger current sink which then grows as CO_2 increases, whereas the emission due to land use changes is initially held constant and later decreases. As long as the sinks which balance net emissions due to deforestation grow faster than the rate of deforestation (which must eventually decrease), these qualitative results will carry over to the real world.

4.3. *Delayed-Action Scenarios*

Table VIII gives peak atmospheric CO_2 concentrations, warming between 1980 and 2025, maximum warming after 1980, and other results for a scenario in which fossil fuel emissions increase by 1% yr^{-1} until 2020, followed by a 1% yr^{-1} decrease after 2030, with alternative assumptions for other trace gases and deforestation: a high trace gas scenario, in which non-CO_2 trace gas variation is the same as in the business-as-usual scenario, and a low trace gas scenario, in which constraints on CH_4, N_2O, and O_3 begin in 2025 as described in Section 3.3, and CFC production is zero after 2003. The two deforestation scenarios are given in Table III, the higher

TABLE VIII: Effects of restrictions on the buildup of non-CO_2 trace gases and on the rate of deforestation, and of uncertainty in the emission due to land use changes. Given are peak atmospheric CO_2 concentration (ppmv), peak CO_2 increase attributable to temperature-pCO_2 feedback (ΔCO_2), warming from 1980–2025 (ΔT_{2025}), peak atmospheric warming ΔT_{max} (°C) after 1980, and maximum rate of global mean warming $(dT/dt)_{max}$ (°C $decade^{-1}$). Also given are cumulative emission due to land use changes and due to biosphere feedback for 1980–2200. The column labelled ΔT_{eq} indicates whether the upwelling-diffusion climate model with low temperature sensitivity (L) or the pure diffusion climate model with high temperature sensitivity (H) is used

Case	ΔT_{eq}	Peak CO_2	ΔCO_2	ΔT_{2025}	ΔT_{max}	$\frac{dT}{dt}$	Land use	Biosphere feedback
	1980 land use emission of 1.0 GT C							
High deforestation and	L	468	34	0.9	1.9	0.21	113	−210
high trace gas	H	483	51	1.2	3.2	0.27	113	−207
low trace gas	L	461	24	0.8	1.1	0.21	113	−211
	H	472	37	1.1	2.0	0.26	113	−208
Low deforestation and	L	447	22	0.8	1.0	0.21	33	−199
low trace gas	H	457	32	1.0	1.9	0.26	33	−196
	1980 land use emission of 2.5 GT C							
Low trace gas and	L	438	23	0.9	1.1	0.23	239	−174
high deforestation	H	444	33	1.2	1.9	0.28	239	−168
low deforestation	L	408	19	0.7	0.8	0.22	89	−147
	H	414	27	1.0	1.6	0.27	89	−142

For all scenarios, 1% yr^{-1} growth of fossil fuel CO_2 emissions is assumed to the year 2020, followed by 1% yr^{-1} decrease after 2030, and $\beta = 0.4$.

of which is the same as in the business-as-usual scenario. Results are given for low (L) and high (H) climate model sensitivities, and for low (1 GT C net in 1980) and high (2.5 GT C net in 1980) land use emissions. A β of 0.4 is assumed in all cases, with an additional sink in 1980 of 0.5 GT C for the low 1980 land use emission and 1.8 GT C for the high 1980 land use emission assumption.

Comparing Tables VI and VIII, it is seen that allowing fossil fuel CO_2 emissions to increase by only 1% yr^{-1} until only 2020, but assuming the same deforestation and trace gas increases as in the business-as-usual scenario, reduces the peak warming after 1980 by over 50%, from 4.4–6.9 °C to 1.9–3.2 °C. Assuming the low rather than the high trace gas scenario reduces the peak warming by a further 0.8–1.2 °C, while assuming the low rather than the high deforestation scenario reduces peak atmospheric CO_2 concentration by about 15 and 30 ppmv for the low and high emission assumptions, respectively, and reduces the peak warming by 0.1–0.3 °C. Altogether, the peak warming after 1980 ranges from 0.8–3.2 °C, while the 1980–2025 warming ranges from 0.7–1.2 °C. Biosphere feedback from CO_2 and temperature increases gives a net sink between 1985–2200 of about 140–210 GT C.

Table IX gives peak atmospheric CO_2 concentrations, maximum warming after 1980, and other results for scenarios in which fossil fuel emissions are constant at their 1986 value or increase by 1% yr^{-1} until either 2000 or 2020, followed by a transition to either a 1% yr^{-1} or 2% yr^{-1} decrease. All cases assume the low trace gas and deforestation scenarios, a land use emission in 1980 of 1.0 GT C, $\beta = 0.4$, and $S_{1980} = 0.5$ GT C yr^{-1}. Results for high trace gas and/or deforestation scenarios can be approximated by adding the differences found in Table VIII to the results given in Table IX.

Allowing CO_2 emissions to grow by 1% yr^{-1} until the year 2000 rather than 2020, following by a 1% yr^{-1} decrease, reduces the peak warming by about 25% (0.3–0.5 °C). Taking a longer transition starting after 2000 but to a rate of decrease of 2% yr^{-1} rather than 1% yr^{-1} reduces the peak warming by a further 15–20% (0.1–0.2 °C), to 0.6–1.2 °C. For low climatic sensitivity, limiting the peak warming after 1980 to 1.0 °C requires no more than 1% yr^{-1} growth in CO_2 emissions until no later than 2020, followed by reduced emissions. For high climatic sensitivity, peak warming can be kept below 1.0 °C only if CO_2 emissions are held constant to 2000, followed by a 10 yr transition to an emission decrease of 2% yr^{-1}. Overall, peak warming ranges from 0.5–2.3 °C while 1980–2025 warming ranges from 0.5–1.2 °C. Peak atmospheric CO_2 concentration ranges from 380 to 457 ppmv. Because of our use of a β of 0.4, the undisturbed biosphere constitutes a net sink of 113–199 GT C between 1985–2200.

Although a β of 0.4 is required in order to reproduce the historical CO_2 increase, this value may not be appropriate in the future because the future response of the biosphere might be more strongly limited by nutrients or by forest dieback due to pollution and rapid climatic change. We therefore test the effect of assuming that the undisturbed biosphere ceases to be a net carbon sink after 1985. Results

TABLE IX: Atmospheric CO_2 concentrations, temperature changes, and other variables for scenarios in which fossil fuel emissions increase by 1% yr^{-1} or are held constant until 2000 or 2020, followed by a transition to a rate of decrease of 1 or 2% yr^{-1}. The low deforestation rate scenario along with CFC production ending by 2003 is assumed in all cases, along with restrictions on the buildup of other greenhouse gases once CO_2 emissions begin to decrease. See caption to Table VIII for explanation of column headings and units

Scenario		ΔT_{eq}	Peak CO_2	ΔCO_2	ΔT_{2025}	ΔT_{max}	$\frac{dT}{dt}$	Land use	Biosphere feedback
+1% to 2020 and									
−1% after 2030	L	447	22	0.8	1.0	0.21	33	−199	
	H	457	36	1.0	1.9	0.26	33	−196	
	H	504	42	1.2	2.3	0.29	33	0	
−2% after 2035	L	427	20	0.8	0.9	0.21	33	−177	
	H	433	30	1.1	1.7	0.26	33	−171	
+1% to 2000 and									
−1% after 2010	L	408	17	0.6	0.7	0.21	33	−155	
	H	415	26	0.9	1.4	0.26	33	−152	
−2% after 2015	L	393	16	0.6	0.6	0.21	33	−136	
	H	398	23	0.9	1.2	0.26	33	−131	
constant to 2020									
−1% after 2025	L	406	18	0.7	0.8	0.20	33	−150	
	H	414	28	1.0	1.5	0.25	33	−147	
−2% after 2030	L	396	17	0.7	0.7	0.20	33	−138	
	H	402	25	1.0	1.3	0.25	33	−133	
constant to 2000									
−1% after 2005	L	392	15	0.5	0.6	0.20	33	−134	
	H	399	23	0.8	1.2	0.25	33	−131	
−2% after 2010	L	380	14	0.5	0.5	0.20	33	−118	
	H	385	21	0.8	1.0	0.25	33	−113	
	H	408	24	0.9	1.3	0.28	33	0	

For all scenarios, $\beta = 0.4$, $S_{1980} = 0.5$ GT C yr^{-1}, land use emission in 1980 is 1.0 GT C, and the low trace gas and deforestation scenarios are assumed.

are given in Table IX for the lowest and highest of the fossil fuel emission scenarios shown in that table. Peak atmospheric CO_2 concentrations are 408 and 504 ppmv for these two cases.[6] Thus, we conclude that, for the range of fossil fuel emission scenarios considered here and assuming the low deforestation scenario, atmospheric CO_2 can be stabilized in the range of 400–500 ppmv – significantly below the doubling level.

Figure 5a gives the CO_2 variation from 1950–2200 for selected scenarios, while figure 5b shows the variation of fossil fuel emission and of the total CO_2 sink (consisting of oceanic uptake, the miscellaneous sink term, and net biospheric uptake due to feedback minus emissions due to land use changes) for two scenarios in

[6] The increase in peak atmospheric CO_2 corresponds to a 45–50% airborne fraction for the CO_2 no longer taken up by the biosphere. The reader can therefore approximate the effect on peak atmospheric CO_2 of alternative biospheric assumptions for the range of fossil fuel emission scenarios considered here.

which fossil fuel CO_2 emissions increase by 1% yr^{-1} until 2020, then decrease by 1% or 2% yr^{-1}. The decrease of sink strength between 1980–1990 reflects an increase in the rate of deforestation, while the strong increase between 1990–2000 reflects a decrease in gross emissions under the low deforestation scenario. Note that these results assume a low 1980 land use net emission of 1.0 GT C; the increase in sink strength after 1990 resulting from reduced rates of deforestation would be even more dramatic assuming higher land use emission.

The difference between the fossil fuel emission rate and total sink strength gives the rate of atmospheric CO_2 increase, and this difference divided by the fossil fuel emission rate gives the instantaneous, apparent fossil fuel airborne fraction. It is readily seen from Figure 5b that the instantaneous airborne fraction decreases rapidly once emissions begin to fall. Both the oceanic uptake and total sink strength

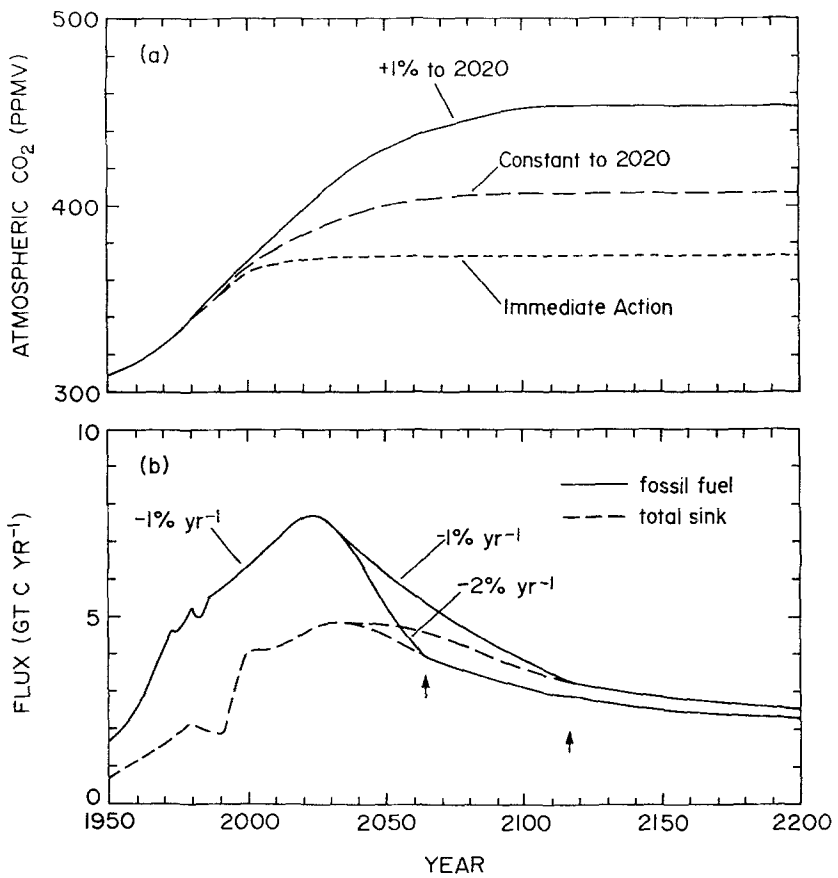

Fig. 5. (a) Atmospheric CO_2 concentration, 1950–2200, for selected emission scenarios. (b) Fossil fuel emissions (solid line) and total sink strength (dashed lines) for scenarios in which fossil fuel emissions increase by 1% yr^{-1} until 2020, then decrease by 1% or 2% yr^{-1}. The low deforestation scenario is assumed, along with a land use emission in 1980 of 1.0 GT C, $\beta = 0.4$, and $S_{1980} = 0.5$ GT C yr^{-1}.

continue to increase for about 15 yrs after peak fossil fuel emissions; under the assumption of constant airborne fraction, the oceanic uptake would start to decrease as soon as emissions decrease. The model behavior seems to be realistic, since even after emissions begin to decrease, atmospheric CO_2 concentration is still increasing rapidly, which in nature would continue to increase the atmosphere-ocean pCO_2 difference and hence the rate of oceanic uptake. The airborne fraction thus falls rapidly because oceanic uptake continues to increase at the same time that emissions decrease.

Once emissions fall to the sink strength, the instantaneous airborne fraction is zero. In the scenarios used here, subsequent emission reductions are tied to the gradual decrease in sink strength, so that the instantaneous airborne fraction remains at zero, and atmospheric CO_2 is stabilized at 430–460 ppmv. Because the behavior of the airborne fraction is so important to the stabilization of atmospheric CO_2 obtained here, analytical solutions for the airborne fraction for the case of exponentially increasing emission followed by a sudden switch to constant emissions are presented and discussed in an Appendix. The results presented here and in the Appendix suggest that it will be considerably easier to prevent atmospheric CO_2 from rising above a given ceiling, such as 500 ppmv, than indicated by previous studies, in which a constant airborne fraction was assumed (Perry *et al.*, 1982; Perry, 1986, Goldemberg *et al.*, 1985, 1988; Mintzer, 1987).

About half of the total sink shown in Figure 5b is due to the miscellaneous sink term and enhanced growth of the undisturbed biosphere. Recall that these sinks are required in order to simulate the historical CO_2 variation in the presence of land use emissions; if these sinks are absent, then the oceanic uptake must be larger, but the effect on future atmospheric CO_2 is similar, as shown for the business-as-usual scenarios (Table VI). These sinks are most likely to persist in the future for small CO_2 increases, such as considered here, and contribute to the stabilization of atmospheric CO_2 at 400–500 ppmv obtained here.

Figure 6 gives the variation of temperature and trace gas radiative forcing for 1950–2200 for a worst case scenario (+2% growth of CO_2 emissions until 2020, high deforestation, high trace gases) and for the Immediate Action scenario, described below. The maximum rate of global mean temperature change is about 0.3° decade^{-1} and occurs between about 1985–1995 for all scenarios given in Table IX. In mid latitudes, where climatic sensitivity is 2 or more times greater than the global mean sensitivity, rates of warming of 0.4–0.6 °C decade^{-1} or more can be expected. Such rates of warming would severely stress forests, particularly those already subject to pollution stress. In reality, short term oscillations superimposed on the warming trend of the magnitude occurring prior to 1985 could halt or reverse the long-term warming trend for one to several decades (as happened between 1940–1960), followed by substantially faster rates of warming than given above.

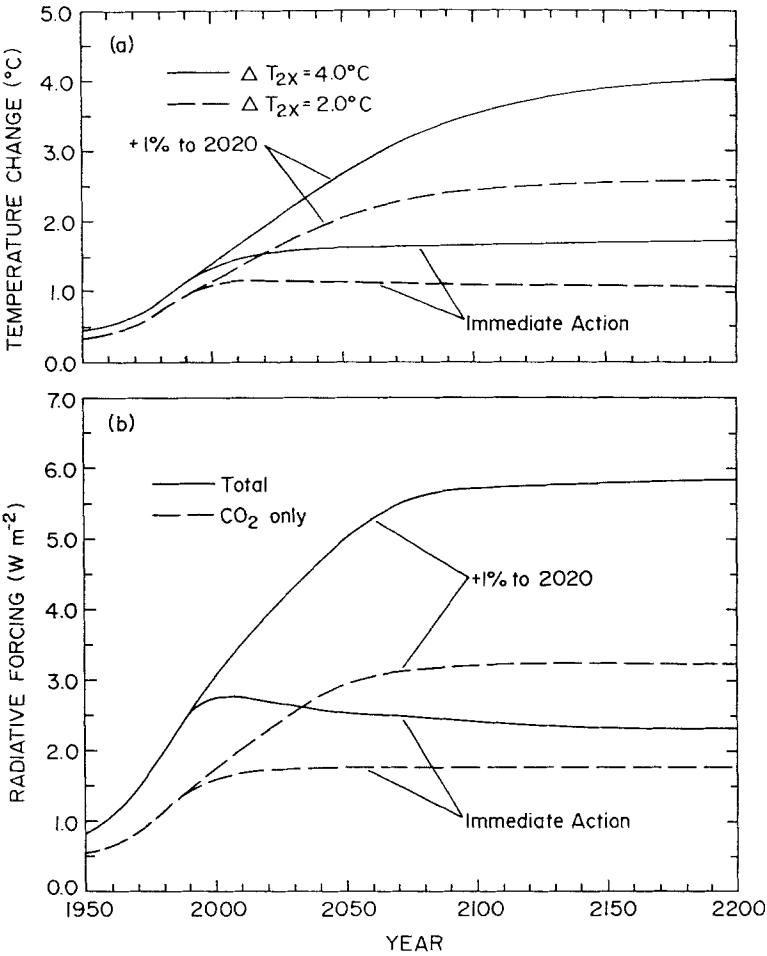

Fig. 6. (a) Atmospheric temperature increase (°C) above the 1770 value for 1950–2200 for the scenario in which fossil fuel CO_2 emissions increase by 2% yr^{-1} until 2020 with high deforestation and trace gases, and for the Immediate Action scenario with low deforestation and trace gases. (b) Radiative forcing (W m^{-2}) due to CO_2 alone and total forcing. A land use emission in 1980 of 1.0 GT C is assumed, along with $\beta = 0.4$ and $S_{1980} = 0.5$ GT C yr^{-1}.

4.4. *Effects of Immediate Action*

In the final set of sensitivity experiments, we consider scenarios in which fossil fuel emissions are reduced by 20% by the year 2005, as recommended by the 1988 Toronto conference *The Changing Atmosphere: Implications for Global Security* (Conference Statement, 1988). Fossil fuel emissions are assumed to be constant from 1986 to 1991, then undergo a transition to $\gamma_2 = 2\%$ yr^{-1} by 2001. As in all other scenarios, this rate of decrease in fossil fuel emissions continues only until the total anthropogenic source equals the total sink, after which a slower rate of decrease is permitted. Temperature and CO_2 results are given in Table X for low

TABLE X: Atmospheric temperature changes and CO_2 concentrations for the Immediate Action scenario. See caption to Table VIII for explanation of column headings and units

Scenario		ΔT_{eq}	Peak CO_2	ΔCO_2	ΔT_{2025}	ΔT_{max}	Land use	Biosphere feedback
		1980 land use emission of 1.0 GT C						
High deforestation and high trace gas	L	394	23	0.8	1.4	113	−125
	H	400	27	1.0	2.5	113	−117
low trace gas	L	390	15	0.5	0.5	113	−126
	H	395	14	0.8	1.1	113	−131
Low deforestation and low trace gas	L	373	13	0.4	0.4	33	−108
	H	377	19	0.7	0.8	33	−104
		1980 land use emission of 2.5 GT C						
Low trace gas and high deforestation	L	390	15	0.5	0.6	239	−123
	H	394	24	0.8	1.2	239	−118
low deforestation	L	366	13	0.4	0.4	89	−96
	H	368	19	0.6	0.8	89	−89

For all scenarios, $\beta = 0.4$.

and high trace gas scenarios and for low and high deforestation scenarios.

Peak atmospheric CO_2 concentration ranges from about 370–400 ppmv. Atmospheric CO_2 stops rising by about 2002 to 2051, depending on the deforestation scenario and associated emissions, at which point fossil fuel emissions are 2.0–

TABLE XI: Permitted fossil fuel emissions (GT C yr^{-1}) at selected years for the Immediate Action scenario and for scenarios in which fossil fuel CO_2 emissions are constant until 2000 or 2020, then decrease by 1% or 2% yr^{-1} until fossil fuel emissions equal the CO_2 uptake by the oceans and other sinks, after which fossil fuel emissions are tied to the gradually decreasing sink strength

		Constant CO_2 emissions until:			
	1991 (IA)	2000 followed by:		2020	
Year	−2% yr^{-1}	−1% yr^{-1}	−2% yr^{-1}	−1% yr^{-1}	−2% yr^{-1}
2050	2.2	3.6	2.5	4.3	3.5
2100	1.9	2.4	2.0	2.7	2.4
2150	1.7	2.1	1.8	2.3	2.1
2200	1.6	1.9	1.7	1.9	1.9
Year emissions tied to oceanic uptake:	2038	2088	2045	2098	2059
Peak CO_2:	373–377	392–399	380–385	406–414	396–402
Peak ΔT_a:	0.4–0.8	0.6–1.2	0.5–1.0	0.8–1.5	0.7–1.3

4.9 GT C yr^{-1}. Peak warming above the 1980 temperature range from 0.4–0.8 °C for low deforestation and trace gas scenarios, and from 1.4–2.5 °C for high deforestation and trace gas scenarios (Table X). Except for the high trace gas scenario, in which non-CO_2 trace gases continue to increase until 2075, most of the warming has occurred by 2025.

5. Tieing CO_2 Emissions to Oceanic Uptake

Once fossil fuel emissions decrease to the rate of CO_2 uptake by oceanic and other sinks, atmospheric CO_2 could be stabilized by tying subsequent fossil fuel emission reductions to the rate of decrease in total sink strength. Because of the long time constants in the oceanic uptake of CO_2 (Table I), the oceanic uptake falls more slowly than fossil fuel emissions for either a 1% yr^{-1} or 2% yr^{-1} rate of decrease. After about 2050 the biospheric sink also slowly decreases in strength, whereas the miscellaneous sink is constant here. Thus, once fossil fuel emissions drop to the total sink strength, it is possible that subsequent (and possibly more difficult) reductions could proceed more slowly.

Table XI gives the permitted fossil fuel emissions required to stabilize atmospheric CO_2 at the peak value for scenarios in which fossil fuel emissions are constant until 2000 or 2020, and for the Immediate Action scenario. Also given are concentrations at which CO_2 is stabilized, the year at which fossil fuel emissions are tied to oceanic CO_2 uptake, and peak climatic warming. In 2050 the permitted CO_2 emissions are 40–80% of current fossil fuel emissions.

A change in oceanic circulation in response to climatic warming could lead to a further increase of atmospheric CO_2 (Baes, 1982; Broecker and Takahashi, 1985). As an upper limit to the potential magnitude of such a feedback, one can use the most rapid rates of atmospheric CO_2 variation which occurred naturally in the past; this rate is a change of 70 ppmv in perhaps as little as 100 yrs (Stauffer *et al.*, 1984), corresponding to a change in oceanic CO_2 uptake or release of about 1.4 GT C yr^{-1}. Were the oceanic uptake to decrease unexpectedly by this magnitude during the next century, this could be entirely counteracted by reducing CO_2 emissions by 1.4 GT C yr^{-1}. For the permitted CO_2 emissions given in Table XI, this requires reducing CO_2 emissions by 35–70% of what would otherwise be permitted in 2050 while still stabilizing atmospheric CO_2 near 400 ppmv. Reforestation could also be effective in partially counteracting perturbations of this magnitude (Marland, 1988). If human societies decide to dampen rather than entirely counteract any unexpected feedbacks, then smaller CO_2 emission reductions would be required.

6. Discussion and Conclusions

The coupled climate-carbon cycle model on which the present results are based is subject to many uncertainties and limitations. Nevertheless, the results reported

here indicate that if fossil fuel emissions were to begin decreasing by 1–2% yr^{-1} no later than 2020, then atmospheric CO_2 could be stabilized at 400–500 ppmv and global mean climatic warming above 1980 temperatures could be limited to as little as 0.6–1.2 °C.

The most important factor contributing to the stabilization of atmospheric CO_2 at 400–500 ppmv obtained here is the comparatively slow decrease in the strength of the oceanic CO_2 sink after fossil fuel emissions begin to decrease. This causes the airborne fraction to rapidly decrease once emissions begin to decrease, and to eventually fall to zero. The accuracy of the behavior of the airborne fraction obtained here is dependent on the fidelity of the Maier-Reimer and Hasselmann (1987) oceanic GCM, upon which the current model is based. Nevertheless, analytical results presented in the Appendix for the response of the airborne fraction to a sudden switch from exponentially increasing to constant emissions (with the latter equal to the rate of oceanic CO_2 uptake at the time of the switch) indicate that, for any linear model, the airborne fraction will not rise to more than about half the value it had just prior to the switch to constant emissions. Accounting for nonlinear oceanic chemistry or the weak temperature-pCO_2 feedback does not alter this result for the small cumulative CO_2 emissions considered under the delayed action scenarios. Only a significant change in oceanic circulation could cause the airborne fraction to return to the value it had during the period of exponentially increasing emission. However, it is suggested here that the largest plausible perturbation in the atmosphere-ocean CO_2 flux due to ocean-climate feedback – 1.4 GT C yr^{-1} – could be compensated for by an accelerated rate of decrease in fossil fuel emissions, reforestation, or some combination of the two.

Another important factor contributing to the stabilization of atmospheric CO_2 arises from the fact that gross emissions due to deforestation appear to be about twice the net emission. As a result, reducing the rate of deforestation to about half its current rate is sufficient, in the short term, to reduce the net emission from deforestation to about zero.

As in previous studies, a CO_2-fertilization effect is necessary in order to simulate the observed atmospheric CO_2 increase. In most instances, a β value of 0.4 was used. One may question the use of $\beta = 0.4$, but a smaller β necessitates a larger miscellaneous sink to match the historical CO_2 variations, or requires reducing the time constants for oceanic uptake of CO_2, both of which give projected future CO_2 concentrations comparable to those obtained using $\beta = 0.4$. Assuming that the undisturbed biosphere constituted a net sink up to 1984 with $\beta = 0.4$ but ceases to be either a sink or a source after 1984 still gives a peak atmospheric CO_2 of 400–500 ppmv for the range of scenarios considered here. The results obtained here indicate that there is a large window of opportunity concerning future atmospheric CO_2 and climatic warming, and should dispel notions that a CO_2 doubling is unavoidable.

The temperature and CO_2 results presented in this paper include the effect of concurrent increases in non-CO_2 trace gases, but assume that these gases are stabi-

lized or undergo a modest decrease once measures are taken to reduce CO_2 emissions. Not accounted for are possible positive feedbacks involving the release of CH_4 from marine clathrate (Bell, 1982) or through enhanced biological activity (Guthrie, 1986), and additional CO_2 emissions from the terrestrial biosphere during the transient due to forest dieback associated with rapid climatic change (Solomon, 1986). The risk posed by these possible feedbacks underlines the importance of early actions to reduce the buildup of greenhouse gases.

Elsewhere (Harvey, 1989d), sets of assumptions under which fossil fuel emission reduction rates of 1–2% yr^{-1} could be achieved are investigated. The sets of assumptions considered pertain to (i) population growth and per capita primary energy demand in the industrialized and developing countries, (ii) rates of introduction of non-fossil fuel energy supplies, and (iii) the mix of fossil fuels used. In that study, global population is assumed to reach 8–10 billion by 2100, industrialized country per capita primary energy demand decreases by 15–45% from its 1980 value, and third world per capita primary commercial energy demand increases by 120–340%. It is also assumed, based on analyses in Goldemberg *et al.* (1985, 1988), that a rate of installation of non-fossil fuel power supply of 150 GW yr^{-1} is achievable. Under these assumptions, and with policy measures starting in 2000, the year in which a target CO_2 emission reduction rate of 1% yr^{-1} is achieved ranges from 2014 to 2093, while a target CO_2 emission reduction rate of 2% yr^{-1} is achieved as early as 2033. The calculated fossil fuel CO_2 emissions, combined with the high deforestation scenario, give peak atmospheric CO_2 concentrations of 400–500 ppmv when used as input to the model described here. Therefore, based on the results presented here and in Harvey (1989d), it is concluded that limiting atmospheric CO_2 to 400–500 ppmv is a credible option.[7]

Acknowledgements

I would like to thank C. Covey, J. Firor, C. Hall, F. K. Hare, M. I. Hoffert, J. A. Laurmann, M. E. Schlesinger, S. H. Schneider, U. Siegenthaler, T. M. L. Wigley, and T. Volk for their helpful comments on earlier versions of this paper. I would also like to thank C. Hall for testing the effect in his land use model of a number of scenarios of future rates of deforestation. This work was supported by Natural Sciences and Engineering Research Council of Canada Grant OPG0001413 and made use of the Ontario Centre for Large Scale Computation Cray XMP-24.

[7] For those wishing to carry out further sensitivity studies, an extensively documented FORTRAN code of the climate-carbon cycle model used here and of the CO_2 emission model used in Harvey (1989d) is available upon request. Requests can be sent by electronic mail to harvey@geog.utoronto.ca, or by regular mail if accompanied by a 5 inch floppy diskette.

Appendix

A feature of the carbon cycle model used here which is of critical importance to policy options for limiting the buildup of, and eventually stabilizing, atmospheric CO_2 is the behavior of the atmospheric airborne fraction. The airborne fraction is given by the difference between total emissions and the total uptake by CO_2 sinks during a given time interval, divided by the emissions during that interval. If anthropogenic CO_2 emissions can be reduced rapidly enough to reach the changing rate of CO_2 uptake by the oceans and other sinks, the airborne fraction will, by definition, be zero. The model results presented here indicate that, once emissions have been reduced to the rate of CO_2 uptake by the sinks, subsequent emission reductions could proceed more slowly, as the rate of oceanic absorption gradually decreases, and still maintain an airborne fraction of zero.

Because the behavior of the airborne fraction is so important to the model atmospheric CO_2 response, we analyze one further, idealized scenario, in which fossil fuel emissions suddenly drop to the rate of oceanic CO_2 absorption in 1990 and are held constant thereafter. The convolution integral (Equation 4) used here to model oceanic CO_2 uptake includes the effects of non-linear oceanic chemistry through the use of impulse response functions G_1, G_2, and G_3 corresponding to successively larger cumulative CO_2 injections. We now consider two cases, one in which G_1 is used at all times, and another in which we switch from G_1 to G_2 in 1990. These shall be referred to as the linear and non-linear cases, respectively. The non-linear case enhances the increase in the airborne fraction following the reduction of CO_2 emissions. For both cases, biospheric CO_2 exchange with the atmosphere and oceanic temperature-pCO_2 feedback are suppressed.

Figure A1 shows the variation from 1950 to 2100 of fossil fuel emissions and oceanic uptake of CO_2 for the linear and non-linear cases. The airborne fraction is about 0.6 just before the switch to constant emissions, falls to zero when emissions are reduced to the rate of oceanic uptake, then slowly rises to a maximum value of 0.28 and 0.32 about 40 yrs after the switch to constant emissions for the linear and non-linear cases, respectively. This is followed by a very gradual decline.

To gain further insight into this behaviour, we examine analytic solutions to Equation (2) using the single impulse response function G_1. Table AI gives solutions for exponentially increasing emissions, for constant emissions, and for exponentially increasing emissions up to time t_1 followed by constant emissions. The instantaneous airborne fraction, $i(t)$, can be computed from these solutions as the increase of atmospheric CO_2 dy during an infinitesimally small time interval dt, divided by the emission during that time interval. Solutions for $i(t)$ are also given in Table A1. It is seen from Table A1 that as $t \rightarrow \infty$, $i(t)$ for emissions growing exponentially with $e^{\alpha t}$ tends to

$$A_0 + \Sigma A_i(\alpha/(\alpha + 1/\tau_i)), \tag{A1}$$

while for constant emissions, $i(t)$ tends to A_0. For constant emissions at a rate x_1

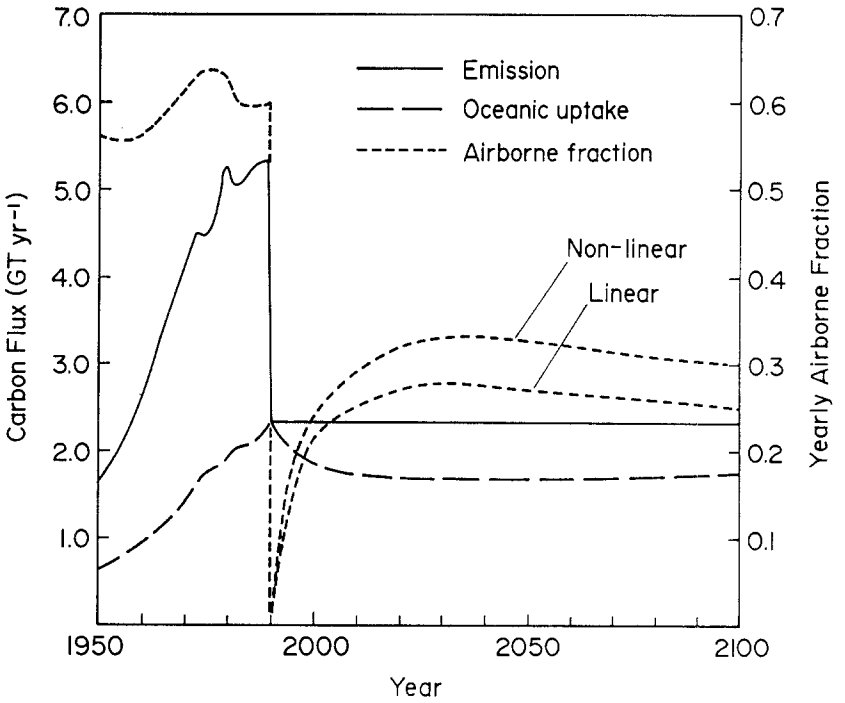

Fig. A1. Variation of fossil fuel emission, oceanic uptake of CO_2, and yearly airborne fraction for a scenario in which fossil fuel emissions are suddenly set to the rate of oceanic uptake in 1990 and held constant. Biosphere feedbacks, land use emissions, and ocean temperature-pCO_2 feedback are suppressed.

after a period of exponentially increasing emissions, $i(t)$ also tends to A_0, irrespective of the value of α, x_1, or t_1. Thus, for linear models, the airborne fraction will always asymptote at a *smaller* value than occurred just before the transition from exponentially increasing to constant emissions.

If we let x_1 equal the rate of oceanic uptake at time t_1, then

$$x_1 = x_0 e^{\alpha t_1}(1 - A_0) - x_0 \Sigma A_i (1/(\alpha + 1/\tau_i)(\alpha e^{\alpha t_1} + (1/\tau_i)e^{-t_1/\tau_i}) . \qquad \text{(A2)}$$

Evaluating the solution for $i(t)$ given in Table AI for the case of exponentially increasing emission followed by constant emissions, with x_1 given by Equation (A2), confirms the behaviour of the airborne fraction shown in Figure A1: $i(t)$ first falls to zero, rises to a maximum, then gradually declines to an asymptotic value of A_0. Table AII gives the asymptotic airborne fraction for emissions increasing exponentially at rates of 1 to 5% yr^{-1}, the value of $i(t)$ the instant before the switch from exponentially increasing emissions to constant emissions given by Equation (A2), the subsequent maximum value of $i(t)$, $i(t)_{max}$, and the number of yrs N after the switch to constant emissions when $i(t)_{max}$ occurs. In every case, $i(t)_{max}$ is about half the value of $i(t)$ just before the switch to constant emissions, while N decreases from 70 yrs for an initial 1% yr^{-1} growth to 39 yrs for 5% yr^{-1} initial growth.

TABLE A1: Analytic solution for atmospheric CO_2 concentration, $y(t)$ and instantaneous airborne fraction, $i(t)$, for various emission scenarios

$x(t)$	$y(t)-y(0)$	$i(t)$
$x_0 e^{\alpha t}$	$\frac{A_0 x_0}{\alpha}(e^{\alpha t}-1)+x_0\Sigma A_i\left(\frac{1}{\alpha+1/\tau_i}\right)(e^{\alpha t}-e^{-t/\tau_i})$	$A_0+e^{-\alpha t}\Sigma A_i\left(\frac{1}{\alpha+1/\tau_i}\right)(\alpha e^{\alpha t}+\frac{1}{\tau_i}e^{-t/\tau_i})$
x_1	$A_0 x_0 t+x_0\Sigma\tau_i A_i(1-e^{-t/\tau_i})$	$A_0+\Sigma A_i e^{-t/\tau_i}$
$x_0 e^{\alpha t}$, $t<t_1$	see case 1 for $t\leqslant t$,	see case 1 for $t\leqslant t_1$
$x_1 \quad t\geqslant t_1$	$\frac{A_0 x_0}{\alpha}(e^{\alpha t_1}-1)+x_0\Sigma A_i\left(\frac{1}{\alpha+1/\tau_i}\right)e^{-t/\tau_i}(e^{-(\alpha+1/\tau_i)t_1}-1)$	$A_0+\Sigma A_i e^{-(t-t_1)/\tau_i}$
	$+A_0 x_1(t-t_1)+x_1\Sigma\tau_i A_i(1-e^{-(t-t_1)/\tau_i}), \quad t>t_1$	$+\frac{x_0}{x_1}\Sigma A_i\left(\frac{1}{\alpha+1/\tau_i}\right)\frac{e^{-t/\tau_i}}{\tau_i}(1-e^{(\alpha+1/\tau_i)}), \quad t>t_1$

TABLE A2: Airborne fractions for fossil fuel emissions increasing exponentially at X% per year until a value of 6.0 GT C yr^{-1} is attained, at time t_1, followed by a sudden switch to an emission rate equal to the rate of oceanic CO_2 uptake at time t_1 and held constant thereafter: Asymptotic airborne fraction for exponentially increasing fossil fuel emissions, $i(\infty)_{exp}$; airborne fraction just before the switch to constant emissions, $i(t_1)$; peak airborne fraction after time t_1, $i(t)_{max}$, and asymptotic airborne fraction for constant emissions, $i(\infty)_{const}$. Also given is the time N in years from t_1 to $i(t)_{max}$

X	$i(\infty)_{exp}$	$i(t_1)$	$i(t)_{max}$	$i(\infty)_{const}$	N
1	0.462	0.463	0.218	0.131	70
2	0.565	0.565	0.258	0.131	53
3	0.624	0.625	0.283	0.131	46
4	0.665	0.665	0.301	0.131	42
5	0.695	0.695	0.315	0.131	39

If effects of non-linear chemistry are accounted for by using impulse functions corresponding to successively larger CO_2 injections as the cumulative emission increases, then the appropriate value of A_0 increases. This causes both $i(t)_{max}$ and the subsequent asymptotic value of $i(t)$ to increase. As illustrated in Figure A1, this non-linear effect is not large. In going from an injection of 0.25 to 3.0 times present CO_2, A_0 for the Maier-Reimer and Hasselmann (1987) model increases from 0.131 to only 0.166 (Table I). The behavior of this model, which we mimic through Equation (4), is thus such that $i(t)_{max}$ following a switch from exponentially increasing to constant emissions given by Equation (A2) will always be less than that during the period of exponentially increasing emissions, with the asymptotic value being even smaller.

For $i(t)$ to rise to, say, 0.5 following a switch to constant emissions requires that the current airborne fraction be larger than 0.5 – something difficult to reconcile with fossil fuel emission, deforestation, and atmospheric CO_2 increase data. The airborne fraction could nevertheless return to its previous value after the switch to constant emissions if there is a sufficiently large change in oceanic circulation or mixing *and* if such changes act as a positive feedback on atmospheric CO_2. The sign of any such feedback is as yet unclear, and the analysis presented in the body of this paper suggests that human societies could compensate for any such positive feedback *if* the current increase in anthropogenic CO_2 emissions is reversed within the next 2–3 decades.

References

Andreae, M. O., Browell, E. V., Garstang, M., Gregory, G. L., Harriss, R. C., Hill, G. F., Jacob, D. J., Pereira, M. C., Sachse, G. W., Setzer, A. W., Silva Dias, P. L., Talbot, R. W., Torres, A. L., and Wofsy, S. C.: 1988, 'Biomass-burning Emissions and Associated Haze Layers over Amazonia', *J. Geophys. Res.* **93**, 1509–1527.

Bacastow, R. B. and Keeling, C. D.: 1973, 'Atmospheric Carbon Dioxide and Radiocarbon in the Natural Carbon Cycle: II. Changes from A.D. 1700 to 2070 as Deduced from a Geochemical Model', in Woodwell, G. M., and Pecan, E. V. (eds.), *Carbon and the Biosphere*, CONF-720510, National Technical Information Service, Springfield VA, USA, 86–135.

Bacastow, R. B. and Bjorkstrom, A.: 1981, 'Comparison of Ocean Models for the Carbon Cycle', in Bolin, B. (ed.), *Carbon Cycle Modelling*, SCOPE 16, John Wiley, Chichester, 29–79.

Baes, C. F.: 1982, 'Ocean Chemistry and Biology', in Clark, W. C. (ed.), *Carbon Dioxide Review: 1982*, Clarendon Press, Oxford, 187–211.

Baes, C. F., Bjorkstrom, A., and Mulholland, P. J.: 1985, 'Uptake of Carbon Dioxide by the Oceans', in Trabalka, J. R. (ed.), *Atmospheric Carbon Dioxide and the Global Carbon Cycle*, U.S. Dept. Energy, DOE/ER-0239, Washington, 81–111.

Baes, C. F. and Killough, G. G.: 1986, 'Chemical and Biological Processes in CO_2-ocean Models', in Trabalka, J. R. and Reichle, D. E. (eds.), *The Changing Carbon Cycle: A Global Analysis*, Springer-Verlag, New York, 329–347.

Bell, R. P.: 1982, 'Methane Hydrate and the Carbon Dioxide Question', in W. C. Clark (ed.), *Carbon Dioxide Review: 1982*. Clarendon Press, Oxford, 401–406.

Bjorkstrom, A.: 1986, 'One-dimensional and Two-dimensional Ocean Models for Predicting the Distribution of CO_2 between the Ocean and Atmosphere', in Trabalka, J. R. and Reichle, D. E. (eds.), *The Changing Carbon Cycle: A Global Analysis*, Springer-Verlag, New York, 258–278.

Broecker, W. S. and Takahashi, T.: 1985, 'Is there a Tie between Atmospheric CO_2 Content and Ocean Circulation?', in Sundquist, E. T. and Broecker, W. S. (eds.), *The Carbon Cycle and Atmospheric CO_2: Natural Variations Archean to Present*, American Geophysical Union, Washington, 314–326.

Brown, S. and Lugo, A. E.: 1982, 'The Storage and Production of Organic Matter in Tropical Forests and their Role in the Global Carbon Cycle', *Biotropica* **14**, 161–187.

Brown, S. and Lugo, A. E.: 1984, 'Biomass of Tropical Forests: A New Estimate Based on Volume', *Science* **22**, 1290–1293.

Chandler, W.: 1988, 'Assessing Carbon Emission Control Strategies: The Case of China', *Clim. Change* **13**, 241–265.

Cheng, H. C., Steinberg, M., and Beller, M.: 1986, *Effects of Energy Technology on Global CO_2 Emissions*, U.S. Dept. Energy, DOE/NBB-0076, Washington, 92 pp.

Conference Statement: 1988, *The Changing Atmosphere: Implications for Global Security*, Environment Canada, Ottawa, 12 pp.

Detwiler, R. P. and Hall, C. A. S.: 1988, 'Tropical Forests and the Global Carbon Cycle', *Science* **239**, 42–47.

Dickinson, R. E. and Cicerone, R. J.: 1986, 'Future Warming from Atmospheric Trace Gases', *Nature* **319**, 109–115.

Edmonds, J. A., Reilly, J. M., Gardner, R. H., and Brenkert, A.: 1986, *Uncertainty in Future Global Energy Use and Fossil Fuel CO_2 Emissions 1975 to 2075*, U.S. Dept. Energy, DOE/NBB-0081, Washington.

Ekdahl, C. A. and Keeling, C. D.: 1973, 'Atmospheric Carbon Dioxide and Radiocarbon in the Natural Carbon Cycle: I. Quantitative Deductions from Records at Mauna Loa Observatory and at the South Pole', in Woodwell, G. M. and Pecan, E. V. (eds.), *Carbon and the Biosphere*, USAEC, 51–85.

Emanuel, W. R., Killough, G. G., Post, W. M., and Shugart, H. H.: 1984, 'Modeling Terrestrial Ecosystems in the Global Carbon Cycle with Shifts in Carbon Storage Capacity by Land-use Change', *Ecology* **65**, 970–983.

Emanuel, W. R., Fung, I. Y.-S., Killough, G. G., Moore, B., and Peng, T.-H.: 1985, 'Modeling the Global Carbon Cycle and Changes in the Atmospheric Carbon Dioxide Levels', in Trabalka, J. R. (ed.), *Atmospheric Carbon Dioxide and the Global Carbon Cycle*, U.S. Dept. Energy, DOE/ER-0239, Washington, 141–173.

Fearnside, P. M.: 1985, 'Brazil's Amazon Forest and the Global Carbon Problem', *Interciencia* **10**, 179–186.

Fearnside, P. M.: 1986, 'Brazil's Amazon Forest and the Global Carbon Problem: Reply to Lugo and Brown', *Interciencia* **11**, 58–64.

Firor, J.: 1988, 'Public Policy and the Airborne Fraction-Guest Editorial', *Clim. Change* **12**, 103–105.

Gaffin, S. R., Hoffert, M. I., and Volk, T.: 1986, 'Nonlinear Coupling between Surface Temperature and Ocean Upwelling as an Agent in Historical Climate Variations', *J. Geophys. Res.* **91**, 3944–3950.

Gammon, R. H., Sundquist, E. T., and Fraser, P. J.: 1985, 'History of Carbon Dioxide in the Atmosphere', in Trabalka, J. R. (ed.), *Atmospheric Carbon Dioxide and the Global Carbon Cycle*, U.S. Dept. Energy, DOE/ER-0239, Washington, 25–62.

Gates, D. M.: 1985, 'Global Biospheric Response to Increasing Atmospheric Carbon Dioxide Concentration', in Strain, B. R. and Cure, J. D. (eds.), *Direct Effects of Increasing Carbon Dioxide on Vegetation*, U.S. Dept. Energy, DOE/ER-0238, Washington, 171–184.

Gifford, G. M.: 1980, 'Carbon Storage by the Biosphere', in Pearman, G. I. (ed.), *Carbon Dioxide and Climate: Australian Contributions*, Australian Academy of Science, Canberra, 167–181.

Gilliland, R. L. and Schneider, S. H.: 1984, 'Volcanic, CO_2, and Solar Forcing of Recent Climatic Changes', *Nature* **310**, 38–41.

Goldemberg, J., Johansson, T. B., Reddy, A. K. N., and Williams, R. H.: 1985, 'An End-use Oriented Global Energy Strategy', *Ann. Rev. Energy* **10**, 613–688.

Goldemberg, J., Johansson, T. B., Reddy, A. K. N., and Williams, R. H.: 1988, *Energy for a Sustainable World*, Wiley Eastern, New Delhi, 517 pp.

Goudriaan, J. and Ketner, P.: 1984, 'A Simulation Study for the Global Carbon Cycle, Including Man's Impact on the Biosphere', *Clim. Change* **6**, 167–192.

Goudriaan, J.: 1989, 'Modelling Biospheric Control of Carbon Fluxes between Atmosphere, Ocean and Land in View of Climatic Change', in Berger, A., Schneider, S. and Duplessy, J. C. (eds.), *Climate and the Geosciences*, NATO ASI, Kluwer Academic Publishers, Dordrecht, The Netherlands, pp. 481–489.

Guthrie, P. D.: 1986, 'Biological Methanogenesis and the CO_2 Greenhouse Effect', *J. Geophys. Res.* **91**, 10847–10851.

Hafele, W.: 1981, *Energy in a Finite World: A Global Systems Analysis*, Ballinger, Cambridge, 837 pp.

Hansen, J. and Lebedeff, S.: 1988, 'Global Surface Air Temperatures: Update through 1987', *Geophys. Res. Let.* **15**, 323–326.

Harvey, L. D. D. and Schneider, S. H.: 1985, 'Transient Climatic Response to External Forcing on 10^0–10^4 Year Time Scales. Part I: Experiments with Globally-averaged Coupled Atmosphere and Ocean Energy Balance Models', *J. Geophys. Res.* **90**, 2191–2205.

Harvey, L. D. D.: 1986, 'Effect of Ocean Mixing on the Transient Response to a CO_2 Increase: Analysis of Recent Model Results', *J. Geophys. Res.* **91**, 2709–2718.

Harvey, L. D. D.: 1989a, 'The Potential Role of Integrated Hydrogen Energy Systems in Alleviating the CO_2 Buildup', *Clim. Change* (submitted).

Harvey, L. D. D.: 1989b, 'An Energy Balance Climate Model Study of Radiative Forcing and Temperature Response at 18 Ka BP', *J. Geophys. Res.* **94**, 12873–12884.

Harvey, L. D. D.: 1989c, 'Effect of Model Structure on Response of Terrestrial Biosphere Models to CO_2 and Temperature Increases', *Global Biogeochem. Cycles* **3**, 137–153.

Harvey, L. D. D.: 1989d, 'Managing Atmospheric CO_2: Policy Implications', *Energy* (accepted).

Heimann, M., Keeling, C. D., and Fung, I. Y.: 1986, 'Simulating the Atmospheric Carbon Dioxide Distribution with a Three-dimensional Tracer Model', in Trabalka, J. R. and Reichle, D. E. (eds.), *The Changing Carbon Cycle: A Global Analysis*, Springer-Verlag, New York, 16–49.

Houghton, R. A.: 1986, 'Estimating Changes in the Carbon Content of Terrestrial Ecosystems from Historical Data', in Trabalka, J. R. and Reichle, D. E. (eds.), *The Changing Carbon Cycle: A Global Analysis*, Springer-Verlag, New York, 175–193.

Houghton, R. A., Hobbie, J. E., Melillo, J. M., Moore, B., Peterson, B. J., Shaver, G. R., and Woodwell, G. M.: 1983, 'Changes in Carbon Content of Terrestrial Biota and Soils between 1860 and 1980: A Net Release of CO_2 to the Atmosphere', *Ecol. Mono* **53**, 235–262.

Houghton, R. A., Boone, R. D., Melillo, J. M., Palm, C. A., Woodwell, G. M., Myers, N., Moore III, B., and Skole, D. L.: 1985, 'Net Flux of Carbon Dioxide from Tropical Forests in 1980', *Nature* **316**, 617–620.

Houghton, R. A., Boone, R. D., Fruci, J. R., Hobbie, J. E., Melillo, J. M., Palm, C. A., Peterson, B. J., Shaver, G. R., and Woodwell, G. M., Moore, B., Skole, D. L., and Myers, N.: 1987, 'The Flux of Carbon from Terrestrial Ecosystems to the Atmosphere in 1980 due to Changes in Land Use: Geographic Distribution of the Global Flux', *Tellus* **39B**, 122–139.

Johansson, T. B.: Bodlund, B., and Williams, R. H. (eds.): 1989, *Electricity: Efficient End-use and New Generation Technologies, and their Planning Implications*, Lund University Press, Lund, 960 pp.

Johansson, T. B. and Williams, R. H.: 1987, 'Energy Conservation in the Global Context', *Energy* **12**, 907–919.

Jones, P. D., Wigley, T. M. L., and Wright, P. B.: 1986, 'Global Temperature Variations between 1861 and 1984', *Nature* **322**, 430–434.

Khandani, S. M. H. and Rose, D. J.: 1985, 'Options in Planning Global Energy Strategies', *Energy* **10**, 887–899.

Killough, G. G. and Emanuel, W. R.: 1981, 'A Comparison of Several Models of Carbon Turnover in the Ocean with Respect to their Distribution of Transit Time and Age, and Response to Atmospheric CO_2 and ^{14}C', *Tellus* **33**, 274–290.

Laurmann, J. A. and Spreiter, J. R.: 1983, 'The Effects of Carbon Cycle Model Error in Calculating Future Atmospheric Carbon Dioxide Levels', *Clim. Change* **5**, 145–181.

Lovins, A. B.: 1980, 'Economically Efficient Energy Futures', in Bach, W., Pankrath, J., and Williams, J. (eds.), *Interactions of Energy and Climate*, Reidel, Dordrecht, Holland, 1–31.

Maier-Reimer, E. and Hasselmann, K.: 1987, 'Transport and Storage of CO_2 in the Ocean – an Inorganic Ocean-circulation Carbon Cycle Model', *Climate Dynamics* **2**, 63–90.

Marland, G.: 1988, *The Prospect of Solving the CO_2 Problem Through Global Reforestation*, U.S. Dept. Energy, DOE/NBB-0082, Washington, 66 pp.

Mintzer, I. M.: 1987, *A Matter of Degrees: The Potential for Controlling the Greenhouse Effect*, World Resources Institute, Washington, 60 pp.

Mulholland, P. J. and Elwood, J. W.: 1982, 'The Role of Lake and Reservoir Sediments as Sinks in the Perturbed Global Carbon Cycle', *Tellus* **34J**, 490–499.

Oeschger, H., Siegenthaler, U., Schotterer, U., and Gugelmann, A.: 1975, 'A Box Diffusion Model to Study the Carbon Dioxide Exchange in Nature', *Tellus* **27**, 168–192.

Oeschger, H. and Stauffer, B.: 1986, 'Review of the History of Atmospheric CO_2 Recorded in Ice Cores', in Trabalka, J. R. (ed.), *The Changing Carbon Cycle: A Global Analysis*, Springer-Verlag, New York, 89–108.

Peng, T.-H. and Freyer, H. D.: 1986, 'Revised Estimates of Atmospheric CO_2 Variations Based on the Tree-ring ^{13}C Record', in Trabalka, J. R. (ed.), *The Changing Carbon Cycle: A Global Analysis*, Springer-Verlag, New York, 151–159.

Peng, T.-H., Takahashi, T., Broecker, W. S., and Olafsson, J.: 1987, 'Seasonal Variability of Carbon Dioxide, Nutrients and Oxygen in the North Atlantic Surface Water: Observations and a Model', *Tellus* **39B**, 439–458.

Perry, A. M., Araj, K. J., Fulkerson, W., Rose, D. J., Miller, M. M., and Rotty, R. M.: 1982, 'Energy Supply and Demand Implications of CO_2', *Energy* **7**, 991–1004.

Perry, A. M.: 1986, 'Possible Changes in Future Use of Fossil Fuels to Limit Environmental Effects', in Trabalka, J. R. and Reichle, D. E. (eds.), *The Changing Carbon Cycle: A Global Analysis*, Springer-Verlag, New York, 561–574.

Ramanathan, V., Callis, L., Cess, R., Hansen, J., Isaksen, I., Kuhn, W., Lacis, A., Luther, F., Mahlman, J., Reck, R., and Schlesinger, M.: 1987, 'Climate-chemical Interactions and Effects of Changing Atmospheric Trace Gases', *Rev. Geophys.* **25**, 1441–1482.

Rotty, R. M.: 1980, 'Data for Global CO_2 Production from Fossil Fuels and Cement', in Bolin, B. (ed.), *Carbon Cycle Modelling, Scope 16*, John Wiley, Chichester, 121–125.

Rotty, R. M.: 1987, 'A Look at 1983 CO_2 Emissions from Fossil Fuels (with preliminary data for 1984)', *Tellus* **39B**, 203–208.

Sarmiento, J. L. and Toggweiler, J. R.: 1984, 'A New Model for the Role of the Oceans in Determining Atmospheric pCO_2', *Nature* **308**, 621–624.

Schlesinger, M. E., and Zhao, Z.-C.: 1989, 'Seasonal Climatic Changes Induced by Doubled CO_2 as Simulated by the OSU Atmospheric GCM/Mixed Layer Ocean Model', *J. Climate* **2**, 459–495.

Siegenthaler, U.: 1983, 'Uptake of Excess CO_2 by an Outcrop-diffusion Model of the Ocean', *J. Geophys. Res.* **88**, 3599–3608.

Siegenthaler, U. and Oeschger, H.: 1987, 'Biospheric CO_2 Emissions during the Past 200 Years Reconstructed by Deconvolution of Ice Core Data', *Tellus* **39B**, 140–154.

Solomon, A. M., Trabalka, J. R., Reichle, D. E., and Voorhees, L. D.: 1985, 'The Global Cycle of Carbon', in Trabalka, J. R. (ed.), *Atmospheric Carbon Dioxide and the Global Carbon Cycle*, U.S. Dept. Energy, DOE/ER-0239, Washington, 1–13.

Solomon, A. M.: 1986, 'Transient Response of Forests to CO_2-induced Climate Change: Simulation Modeling Experiments in Eastern North America', *Oecologia* **68**, 567–579.

Stauffer, B., Hofer, H., Oeschger, H., Schwander, J., and Siegenthaler, U.: 1984, 'Atmospheric CO_2 Concentration during the Last Glaciation', *Annals Glac.* **5**, 160–164.

Trabalka, J. R., Edmonds, J. A., Reilly, J. M., Gardner, R. H., and Reichle, D. E.: 1986, 'Atmospheric CO_2 Projections with Globally Averaged Carbon Cycle Models', in Trabalka, J. R. and Reichle, D. E. (eds.), *The Changing Carbon Cycle: A Global Analysis*, Springer-Verlag, New York, 534–560.

United Nations: 1988, *1986 Energy Statistics Yearbook*, United Nations, Dept. of International Economic and Social Affairs, Statistical Office, New York.

United Nations Environment Programme (UNEP): 1987, *Montreal Protocol on Ozone Depleting Substances*.

Viecelli, J. A., Ellsaesser, H. W., and Burt, J. E.: 1981, 'A Carbon Cycle Model with Latitude Dependence', *Clim. Change* **3**, 281–301.

Wang, W.-C., Wuebbles, D. J., Washington, W. M., Isaacs, R. G., and Molnar, G.: 1986, 'Trace Gases and Other Potential Perturbations to Global Climate', *Rev. Geophys.* **24**, 110–140.

Weiss, R. F.: 1981, 'The Temporal and Spatial Distribution of Tropospheric Nitrous Oxide', *J. Geophys. Res.* **86**, 7185–7195.

Wigley, T. M. L.: 1986, 'Relative Contributions of Different Trace Gases to the Greenhouse Effect', *Climate Monitor* **16**, 14–28.

Wigley, T. M. L.: 1987, 'The Effect of Model Structure on Projections of Greenhouse-gas-induced Climatic Change', *Geophys. Res. Let.* **14**, 1135–1138.

Wigley, T. M. L.: 1988, 'Future CFC Concentrations under the Montreal Protocol and their Greenhouse-effect Implications', *Nature* **335**, 333–335.

Wigley, T. M. L.: 1989, 'Climatic Change due to SO_2-derived Cloud Condensation Nuclei', *Nature* (in press).

Wigley, T. M. L. and Raper, S. C. B.: 1987, 'Thermal Expansion of Sea Water Associated with Global Warming', *Nature* **330**, 127–131.

Wilson, C. A. and Mitchell, J. F. B.: 1987, 'A Doubled CO_2 Climate Sensitivity Experiment with a Global Climate Model Including a Simple Ocean', *J. Geophys. Res.* **92**, 13315–13343.

(Received 19 December, 1988; in revised form 18 May, 1989)